UNIVERSITY OF CALIFORNIA

Santa Barbara

Synthesis of Alkoxides, Imidos, Thiolates, and Phosphides of Uranium and Investigation of their Metal Ligand Bonds

A Thesis submitted in partial satisfaction of the

requirements for the degree Master of Science

in Chemistry

by

Edward Louis Paul

Committee in charge:

Professor Trevor W. Hayton, Chair

Professor Peter C. Ford

Professor Susannah L.Scott

Professor Javier Read de Alaniz

September 2016

The thesis of Edward Louis Paul is approved.

_____

Professor Peter C. Ford

_____

Professor Javier Read de Alaniz

_____

Professor Susannah L. Scott

_____

Professor Trevor W. Hayton, Committee Chair

June 2016

Synthesis of Alkoxides, Imidos, Thiolates, and Phosphides of Uranium and Investigation of their Metal Ligand Bonds

Edward Louis Paul

ABSTRACT

Synthesis of Alkoxides, Imidos, Thiolates, and Phosphides of Uranium and Investigation of their Metal Ligand Bonds

by

Edward Louis Paul

Addition of 2 equiv of Ph_3COH to $UO_2[NR_2]_2(THF)_2$ (R = $SiMe_3$) generates the U(VI) bis-alkoxide complex $UO_2(OCPh_3)_2(THF)_2$. Reduction of $UO_2(OCPh_3)_2(THF)_2$ with 2 equiv of KC_8 results in the reduction of the complex to "$U(IV)O_2$" and formation of $KOCPh_3$. Addition of 2 equiv of Ph_3CSH to $UO_2[NR_2]_2(THF)_2$ generates the U(VI) bis-thiolate complex $UO_2(SCPh_3)_2(THF)_2$. The reduction of $UO_2(SCPh_3)_2(THF)_2$ with 2 equiv of KC_8 results in the reduction of the complex to "$U(IV)O_2$" and formation of $KSCPh_3$. Finally, reduction of $UO_2(SCPh_3)_2(THF)_2$ with 1 equiv of Cp^*_2Co results in the reduction of the complex to "$U(IV)O_2$" and formation of $[Cp^*_2Co][SCPh_3]$.

Addition of 1 equiv of 1-azidoadamantane to $U(NR_2)_3$ (R = $SiMe_3$) generates $(AdN)U(NR_2)_3$. The U(V) imido complexes $(AdN)U(NR_2)_3$ and $(RN)U[N(R)_2]_3$, along with the U(V) oxo $(O)U(NR_2)_3$ were characterized utilizing UV-Visible spectroscopy and SQUID magnetometry to quantify the f-orbital participation in the U-N and U-O multiple bonds.

Addition of Se to $[Na(DME)_3][(N(SiMe_3)_2)_2U(\mu\text{-}N)(CH_2SiMe_2\mathit{N}(SiMe_3))U(N(SiMe_3)_2)_2]$ in the presence of 18-crown-6 resulted in the

formation of [Na(18-crown-6)][$(N(SiMe_3)_2)_2U(\mu$-N)(*Se*$CH_2SiMe_2N(SiMe_3))U(N(SiMe_3)_2)_2$]. Addition of Te to [$Na(DME)_3$][$(N(SiMe_3)_2)_2U(\mu$-N)($CH_2SiMe_2N(SiMe_3)$)$U(N(SiMe_3)_2)_2$] in the presence of 18-crown-6 generates Na(18-crown-6)][$(N(SiMe_3)_2)_2U(\mu$-N)(*Te*$CH_2SiMe_2N(SiMe_3))U(N(SiMe_3)_2)_2$]. Treatment of [$Na(DME)_3$][$(N(SiMe_3)_2)_2U(\mu$-N)($CH_2SiMe_2N(SiMe_3)$)$U(N(SiMe_3)_2)_2$] with 1 equiv of 1-azidoadamantane results in the formation of [$Na(DME)_3$][$(N(SiMe_3)_2)_2(C_{10}H_{15}N)U(\mu$-N)($CH_2SiMe_2N(SiMe_3)$)$U(N(SiMe_3)_2)_2$].

Addition of 4 equiv of $LiNHCPh_3$ to UCl_4, along with 1 equiv of I_2 generates $U(NCPh_3)I_2THF_2$. Treatment of UCl_4 with 4 equiv of $LiNHCPh_3$ and 1 equiv of I_2 in the presence of bipyridine (bipy) generates $U(NCPh_3)I_2(bipy)_2$. Addition of 12 equiv of KC_8 to 7 equiv of P_4 in the presence of 18-crown-6 results in $[K(18\text{-crown-}6)]_3[P_7]$. Treatment of $U(NR_2)_3$ with 0.33 equiv of $[K(18\text{-crown-}6)]_3[P_7]$ results in [K(18-crown-6)][$((SiMe_3)_3U)^2(\mu$-η^2:η^2-P_2] . Addition of 0.5 equivalents of $[K(18\text{-crown-}6)]_3[P_7]$ to $U(NR_2)_3$ (R = $SiMe_3$) generates [K(2,2,2-cryptand)][$((SiMe_3)_2U)^2(\mu$-η^5:η^5-P_5].

TABLE OF CONTENTS

Chapter 1 Introduction

1.1 The f-orbitals

Prior to 1945 it was thought that the heaviest elements such as uranium and thorium were transition metals. However after the emergence of the transuranic elements it was found that this was not the case. The transuranic elements were expected to show similar reactivity to their transition metal counterparts. However, it was found that these transuranic elements seemed to favor the trivalent oxidation state, similar to the lanthanides.[1] With this evidence, along with other physiochemical differences between the transition metals and actinides, and the similarities to the lanthanides, the presence of the f-orbitals was established.

The f-shell is composed of seven sub-orbitals that have ungerade symmetry. The f-orbitals can be depicted in two ways, depending on the geometry around the metal center. For complexes containing O_h and T_d symmetry the f-orbitals can be represented in the cubic set (f_{xyz}, $f_{z(x^2-y^2)}$, $f_{x(y^2-z^2)}$, $f_{y(z^2-x^2)}$, f_{z^3}, f_{x^3}, f_{y^3}), while the general set $f_{y(3x^2-y^2)}$, $f_{x(x^2-3y^2)}$, $f_{z(x^2-y^2)}$, f_{xyz}, f_{z^3}, f_{yz^2}, f_{xz^2}) can be used to describe complexes with non-cubic geometries.[2]

The 4f-orbitals in the lanthanides are poorly shielded from the nuclear charge of the nucleus. Due to the poor shielding, the 4f-shell increasingly contracts with increasing atomic number causing the f-orbitals to become more core-like and inactive. This contraction and inactivity of the 4f-orbitals leads to a preference for the trivalent oxidation state in the lanthanides.[3-5] This contraction also affects the actinides and is evident in the later actinides that are predominately trivalent. Due to the contraction, and the large ionic radii, these elements can accommodate large coordination numbers. [6]

Unlike the compact f-orbitals in the lanthanides and late actinides, the 5f-orbitals of the early actinides are less contracted and shielded by the charge of the nucleus. This is predominantly due to the radial expansion of the 5f orbitals, due to relativistic effects, and suggests that they may participate in metal ligand bonding interactions. As the atomic number increases, the average radial velocity within the core orbitals increases, which causes a relativistic increase in the mass of the inner electrons. In heavy elements, this results in a noticeable contraction of the core orbitals, which can provide shielding for the outer orbitals. In the actinides, the 5f-orbitals are more shielded by the core orbitals which causes the 5f-orbitals to be in close energy proximity to the 6d and 7s valence orbitals, making them more chemically accessible.[7,8] This is directly reflected in the range of oxidation states available to the early actinides, An^{n+} (An = U-Pu; n = 3-6).

1.2 Covalency in the Actinides

Understanding the contribution of the 5f-orbitals to bonding and the level of covalency is important to the study and separation of spent nuclear fuel. Spent nuclear fuel contains long lived actinide(III) isotopes that are difficult to separate from lanthanide(III) fission products due to their similar chemical properties and ionic radii. The majority of long-term radiotoxicity of nuclear waste comes from small amounts of Cm, Am, Np, and Pu.[9] The extraction of these elements from nuclear waste is of high interest to the nuclear community. If these minor actinides can be removed from spent nuclear fuel the radiotoxicity of the fuel will be decreased, the amount of waste that needs to be stored long term will be reduced, and the recovered Cm and Am could then be used in transmutation processes.

The expansion of the 5f-orbitals, and their close relative energy to the 6d and 7s orbitals, highly suggests that they may participate in bonding. It has been generally accepted that the 5f-orbital do in fact participate in the bonding of the actinyl ions. The actinyls have the structure of *trans*-AnO_2^{n+} (An = U-Am; n = 1-2), and are characterized by their linear geometries and short, strong An=O bonds. The An=O bonds contain multiple bond character and has participation of both the 6d and 5f valence orbitals as well as the 6p orbital.[10-12] For example in the U=O bonds in uranyl (UO_2^{2+}) it is calculated that there is 35% f-orbital character in the π_u orbital and 20% d character in the π_g orbital.[12]

That said, the extent in which the 6d and 5f orbitals participate in actinide-ligand bonding is not generally well understood.[13] Past studies have described the actinide bonding as more ionic and containing little covalent character, however, more recent work has shown that this may not always be the case.[6] Computational modeling has shown that these bonding interactions have more covalency than previously assumed, however these methods often tend to overestimate the amount of 6d and 5f-orbital participation.[13] Due to these limitations, investigation into the synthesis and properties of 5f complexes has been conducted. Several techniques have been employed to aid in the understanding of 5f systems including X-ray crystallography, synchrotron X-ray diffraction, and K-edge X-ray absorption spectroscopy.[14-18] These techniques have been helpful but they are limited by the complexes which can be utilized. To further understand the 5f-orbitals, new complexes containing new actinide ligand bonds are necessary for study.

The study of uranyl complexes has given a large amount of insight into the 5f orbitals due to the strong uranium-oxygen interactions.[19-24] These strong multiple bonds have more f-orbital character than single bond interactions, making it easier to observe the 5f-orbitals. Due to the stronger f-orbital character in multiple bonds, it was concluded that the study of uranium-heteroatom multiple bonds and uranyl analogues would yield new information in how the 5f-orbitals participate in bonding. To increase the knowledge about f-orbitals several uranyl analogues were synthesized replacing the hard donor oxygen with heavier, softer donor chalcogens.[25] These complexes also showed significant covalency in the multiple bonds. Several of complexes containing actinide-chalcogen multiple bonds have been synthesized and studied, including the recent synthesis of a full series of terminal chalcogenides synthesized by the Hayton group.[26,27] These complexes have provided good insight into how the 5f orbitals interact with these elements. More recent work has focused on expanding uranium-heteroatom multiple bond chemistry to other elements. The synthesis of uranium imido complexes began in 1980's when Gilje and co-workers synthesized the first actinide imido complex $Cp_3UNC(Me)CHP(Ph)_2Me$.[28] Several other uranium imido complexes have been synthesized and studied in the past several decades and have exhibited a fair amount of covalency and f-orbital participation. This research expanded into making imido analogues of uranyl, which were first synthesized by Boncella and co-workers in 2005. [29-31]The exploration of pnictogen multiple bonds have expanded to nitride complexes in recent years. The Hayton group recently published the synthesis of a bridged uranium nitride complex.[32] This bridging nitride was then used to synthesize an oxy-nitrido complex, a nitride substituted analogue of uranyl. In 2013, Liddle and co-workers

reported the synthesis of a terminal uranium nitride complex. [33,34] Recently the Liddle group synthesized a terminal uranium phosphide and it was found that the uranium contribution to the bond had significant f-orbital character.[35]

The synthesis and characterization of complexes with uranium-heteroatom multiple bonds has provided a wealth of knowledge. Because of the possible insights into actinide bonding, my research has focused on the synthesis and characterization of new uranium heteroatom multiple bonds and new routes of synthesis to these complexes.

1.3 General Remarks

This thesis is divided into four chapters and one appendix. A brief description of each chapter is below.

Chapter 2 describes the synthesis and characterization of a uranyl alkoxide complex and a uranyl thiolate complex toward the synthesis of reverse uranyl and a thio-substituted reverse uranyl.

Chapter 3 describes the utilization of UV-Vis/NIR spectroscopy, SQUID magnetometry, and EPR spectroscopy to experimentally quantify the f-orbital participation in uranium heteroatom multiple bonds in $5f^1$ complexes.

Chapter 4 describes the synthesis and reactivity of several uranium pnictogen complexes. The reactivity of a uranium nitride complex is explored and a new uranium bis imido complex is synthesized. New methods of phosphide and phosphinidene synthesis are explored.

1.4 References

(1) Katz, J. J.; Seaborg, G. T.; Morss, L. R. *The Chemistry of the Actinide Elements*, Second. Chapman and Hall: New York, 1986; Vol. 1.

(2) King, R. B. *Inorg. Chem.* **1992**, *31* (10), 1978–1980.

(3) Katz, J. J.; Morss, L. R.; Edelstein, N. M.; Fuger, J. In *The Chemistry of the Actinide and Transactinide Elements*; Morss, L. R., Edelstein, N. M., Fuger, J., Eds.; Springer Netherlands: Dordrecht, 2006; pp 1–17.

(4) Kaltsoyannis, N.; Hay, P. J.; Li, J.; Blaudeau, J.-P.; Bursten, B. E. In *The Chemistry of the Actinide and Transactinide Elements*; Springer Netherlands: Dordrecht, 2010; pp 1893–2012.

(5) Jensen, M. P.; Bond, A. H. *J. Am. Chem. Soc.* **2002**, *124* (33), 9870–9877.

(6) Choppin, G. R. *J. Alloy. Compounds* **2002**, *344*, 55–59.

(7) Tassell, M. J.; Kaltsoyannis, N. *Dalton Trans.* **2010**, *39* (29), 6719–6725.

(8) Kaltsoyannis, N.; Scott, P. *The f elements*; Oxford University Press: New York, 1999.

(9) Lindley, B. A.; Fiorina, C.; Gregg, R.; Franceschini, F.; Parks, G. T. *Progress in Nuclear Energy* **2015**, *85*, 498–510.

(10) Denning, R. G.; Green, J. C.; Hutchings, T. E.; Dallera, C.; Tagliaferri, A.; Giarda, K.; Brookes, N. B.; Braicovich, L. *J. Chem. Phys.* **2002**, *117*, 8008–8020.

(11) Denning, R. *Struct. Bonding* **1992**, *79*, 215–276.

(12) Kaltsoyannis, N. *Inorg. Chem.* **2000**, *39*, 6009–6017.

(13) Kozimor, S. A.; Yang, P.; Batista, E. R.; Boland, K. S.; Burns, C. J.; Clark, D. L.; Conradson, S. D.; Martin, R. L.; Wilkerson, M. P.; Wolfsberg, L. E. *J. Am. Chem. Soc.* **2009**, *131* (34), 12125–12136.

(14) Jensen, M. P.; Bond, A. H. *J. Am. Chem. Soc.* **2002**, *124*, 9870–9877.

(15) Kozimor, S. A.; Yang, P.; Batista, E. R.; Boland, K. S.; Burns, C. J.; Christensen, C. N.; Clark, D. L.; Conradson, S. D.; Hay, P. J.; Lezama, J. S.; Martin, R. L.; Schwarz, D. E.; Wilkerson, M. P.; Wolfsberg, L. E. *Inorg. Chem.* **2008**, *47* (12), 5365–5371.

(16) Graves, C. R.; Vaughn, A. E.; Schelter, E. J.; Scott, B. L.; Thompson, J. D.; Morris, D. E.; Kiplinger, J. L. *Inorg. Chem.* **2008**, *47* (24), 11879–11891.

(17) Minasian, S. G.; Krinsky, J. L.; Arnold, J. *Chem.-Eur. J.* **2011**, *17* (44), 12234–12245.

(18) Mazzanti, M.; Weitzke, R.; Pecaut, J.; Latour, J. M.; Maldivi, P.; Remy, M. *Inorg. Chem.* **2002**, *41* (9), 2389–2399.

(19) Crandall, H. W. *J. Chem. Phys.* **1949**, *17*, 602–606.

(20) Bradley, D. C.; Chatterjee, A. K. *J. Inorg. Nucl. Chem.* **1959**, *12*, 71–78.

(21) McGlynn, S. P.; Smith, J. K.; Neely, W. C. *J. Chem. Phys.* **1961**, *35*, 105–116.

(22) Bombieri, G.; Croatto, U.; Forsellini, E.; Zarli, B.; Graziani, R. *J. Chem. Soc.-Dalton Trans.* **1971**, 560–564.

(23) Taylor, J. C.; Waugh, A. B. *Dalton Trans.* **1977**, No. 17, 1630–1636.

(24) Anderson, R. A. *Inorg. Chem.* **1979**, *18* (1), 209.

(25) Brown, J. L.; Fortier, S.; Wu, G.; Kaltsoyannis, N.; Hayton, T. W. *J. Am. Chem. Soc.* **2013**, *135* (14), 5352–5355.

(26) Smiles, D. E.; Wu, G.; Hayton, T. W. *J. Am. Chem. Soc.* **2014**, *136* (1), 96–99.

(27) Smiles, D. E.; Wu, G.; Hayton, T. W. *Inorg. Chem.* **2014**, *53* (19), 10240–10247.

(28) Cramer, R. E.; Panchanatheswaran, K.; Gilje, J. W. *J. Am. Chem. Soc.* **1984**, *106* (6), 1853–1854.

(29) Hayton, T. W.; Boncella, J. M.; Scott, B. L.; Palmer, P. D.; Batista, E. R.; Hay, P. J. *Science* **2005**, *310* (5756), 1941–1943.

(30) Hayton, T. W.; Boncella, J. M.; Scott, B. L.; Batista, E. R.; Hay, P. J. *J. Am. Chem. Soc.* **2006**, *128* (32), 10549–10559.

(31) Hayton, T. W.; Boncella, J. M.; Scott, B. L.; Batista, E. R. *J. Am. Chem. Soc.* **2006**, *128* (39), 12622–12623.

(32) Fortier, S.; Wu, G.; Hayton, T. W. *J. Am. Chem. Soc.* **2010**, *132* (20), 6888–6889.

(33) King, D. M.; Tuna, F.; McInnes, E. J. L.; McMaster, J.; Lewis, W.; Blake, A. J.; Liddle, S. T. *Nature Chem* **2013**, *5* (6), 482–488.

(34) King, D. M.; McMaster, J.; Tuna, F.; McInnes, E. J. L.; Lewis, W.; Blake, A. J.; Liddle, S. T. *J. Am. Chem. Soc.* **2014**, *136* (15), 5619–5622.

(35) Gardner, B. M.; Balázs, G.; Scheer, M.; Tuna, F.; McInnes, E. J. L.; McMaster, J.; Lewis, W.; Blake, A. J.; Liddle, S. T. *Angew. Chem.-Int. Edit.* **2014**, n/a–n/a.

Chapter 2 Synthesis and Characterization of Uranyl Trityl Alkoxides and Thiolates

2.1 Introduction

The study of uranium heteroatom multiple bonds in recent years has yielded a wealth of information in how f-orbitals interact in bonding different atoms.[1-6] In addition, the study of uranyl and uranyl analogues has led to more information on the covalency of f-orbitals in the actinides. [1,7-11]These studies have shown that f-orbitals in actinides do participate in the π-bonding in the metal ligand multiple bonds.[12] Because of this information there has been a desire to synthesize new complexes containing new actinide ligand multiple bonds to study how the f-orbitals interact in bonds.

Because the study of uranyl has yielded a wealth of knowledge regarding the f-orbitals it has been proposed that studying systems that contain more than two uranium heteroatom multiple bonds would be fruitful as well. Recent work has succeeded in synthesizing complexes that contain three multiple bonds to heteroatoms.[13] The Bart group in collaboration with the Schelter group synthesized a uranium tris(imido complex). Upon reacting uranium tris-iodide with diisopropylphenyl (DIPP) azide in the presence of KC_8, they synthesized the uranium tris(imido) complex (eq 2.1).[14] In this complex the imido ligands are coordinated in a facial orientation and not a uranyl like structure as would be desired. To remedy this a pyridine(diimine) (PDI) ligand was used to create a uranyl like environment about the uranium center.[15]

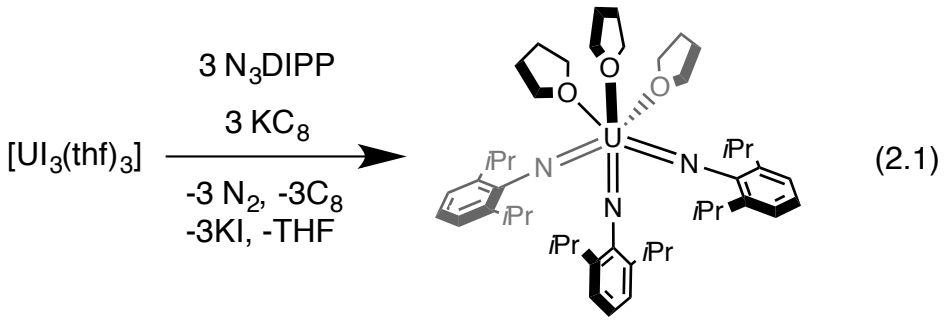

(2.1)

Having observed the synthesis of these complexes, we endeavored to synthesize new uranium complexes containing more than two multiple bonds. The target complex that was selected was the complex known as "reverse uranyl" that has only been observed in the solid state. [16] Reverse uranyl describes a complex that contains four short multiple bonds in an equatorial plane and two long single bonds in an axial position. This would be the direct opposite of uranyl, which contains two short multiple bonds in the axial position and four long single bonds in the equatorial plane.[17,18] Reverse uranyl would be a dianionic compound which was previously thought to be too unstable, but calculations have shown this to be a feasible, somewhat stable product.[19] This complex has been studied theoretically; it has been observed in the solid state however, a discrete independent molecule has not yet been synthesized to confirm the theoretical structure.

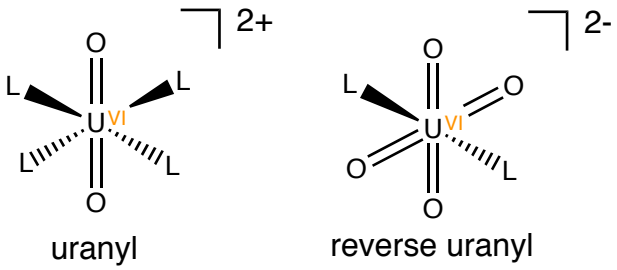

Scheme 1:Structure of Uranyl and Reverse Uranyl

It has been recently hypothesized that the reverse uranyl may in fact distort into a tetrahedral environment instead of the previously hypothesized square planar geometry.[20] To explore the electronic structure and compare it to the proposed configuration we endeavored to synthesize this reverse uranyl.

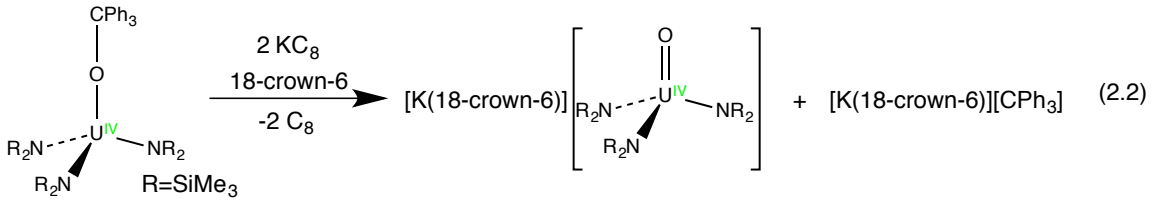

(2.2)

To synthesize reverse uranyl, we chose to utilize the method of reductive deprotection that has been used previously to synthesize several complexes containing metal heteroatom multiple bonds.[21] This method utilized the reductive bond cleavage of a bond between a protecting group and a heteroatom to form a metal heteroatom multiple bond. In the previous work by the Hayton group, the protecting group that was utilized was the triphenylmethyl group (eq 2.2.). Our objective is to first synthesize the uranyl alkoxide complex then reduce the complex and form reverse uranyl.

Uranium alkoxide complexes have been studied for several decades and Gillman and coworkers first reported the preparation of uranium alkoxides and later Bradley and coworkers reported more uranium alkoxide complexes.[16,22-27] Uranyl alkoxide complexes can be made through either a salt metathesis or a ligand metathesis. The salt metathesis method utilizes a halide complex of uranyl and an alkali metal complex of the alkoxide ligand.[28] This method produces the corresponding salt and the desired alkoxide. However there is often the formation of a uranyl tris(alkoxide) ate complex. The second method utilizes a ligand metathesis. This method utilizes a metathesis with a uranyl amide complex and the desired alcohol. This reaction forms the desired alkoxide complex and an amine as the byproduct (eq 2.3).[29] This method is preferred due to the lack of possible byproducts from the reaction mixture.

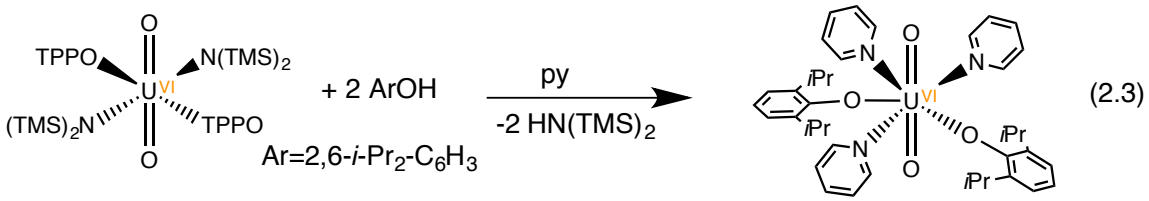

(2.3)

In this chapter the synthesis of the uranyl alkoxide, $UO_2(OCPh_3)_2THF_2$ is discussed as well as the synthesis of the uranyl thiolate complex $UO_2(SCPh_3)_2THF_2$. The reactivity of these complexes toward several reducing agents is explored. The behavior of these complexes toward reducing agents is probed and the deviation from the expected reactivity is discussed.

2.2 Results and Discussion

2.2.1 Synthesis and Characterization of $UO_2(OCPh_3)_2(THF)_2$ (2.1)

Addition of 2 equivalents of Ph_3COH to a solution of $UO_2[N(SiMe_3)_2]_2(THF)_2$ in diethyl ether produces an orange solution from which a yellow precipitate forms. Upon decanting the supernatant, the yellow solid $UO_2(OCPh_3)_2(THF)_2$ (**2.1**) can be isolated in 81% yield (eq 2.4). Re-dissolution of the yellow solid in THF and diffusion of hexanes at -25 °C affords single crystals of **2.1** as yellow plates.

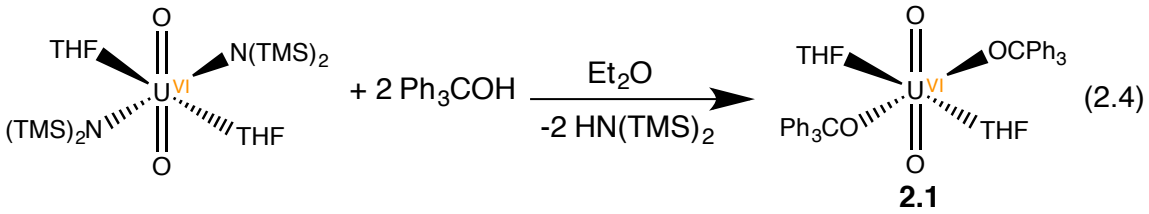

(2.4)

2.1

Complex **2.1** crystallizes in the monoclinic space group $P2_1/n$, and its solid state structure is shown in Figure 2.1. In the solid state, complex 2.1 displays an octahedral environment about the uranium center (O1-U1-O1 = 180.0°). The alkoxide ligands are in the trans configuration as opposed to a cis conformation. Both THF molecules are coordinated to the metal center.

In complex **2.1**, several of the bonds are grown by symmetry due to the space group of the molecule. The uranyl bond distances are both 1.791(5) Å, which is typical for uranyl bond distances.[30,31] The uranium alkoxide bond distances are 2.137(6) Å, which is very similar to the uranyl bis(triphenylphosphine oxide) (TPPO) bis t-butyl alkoxide synthesized by Burns and co-workers, which has an $U\text{-}O_{Alkoxide}$ bond distance of 2.143(6) Å.[28] The coordination environment of the alkoxide and coordinating solvent around the uranyl is typical of $UO_2R^1{}_2R^2{}_2$ complexes with monodentate ligands.

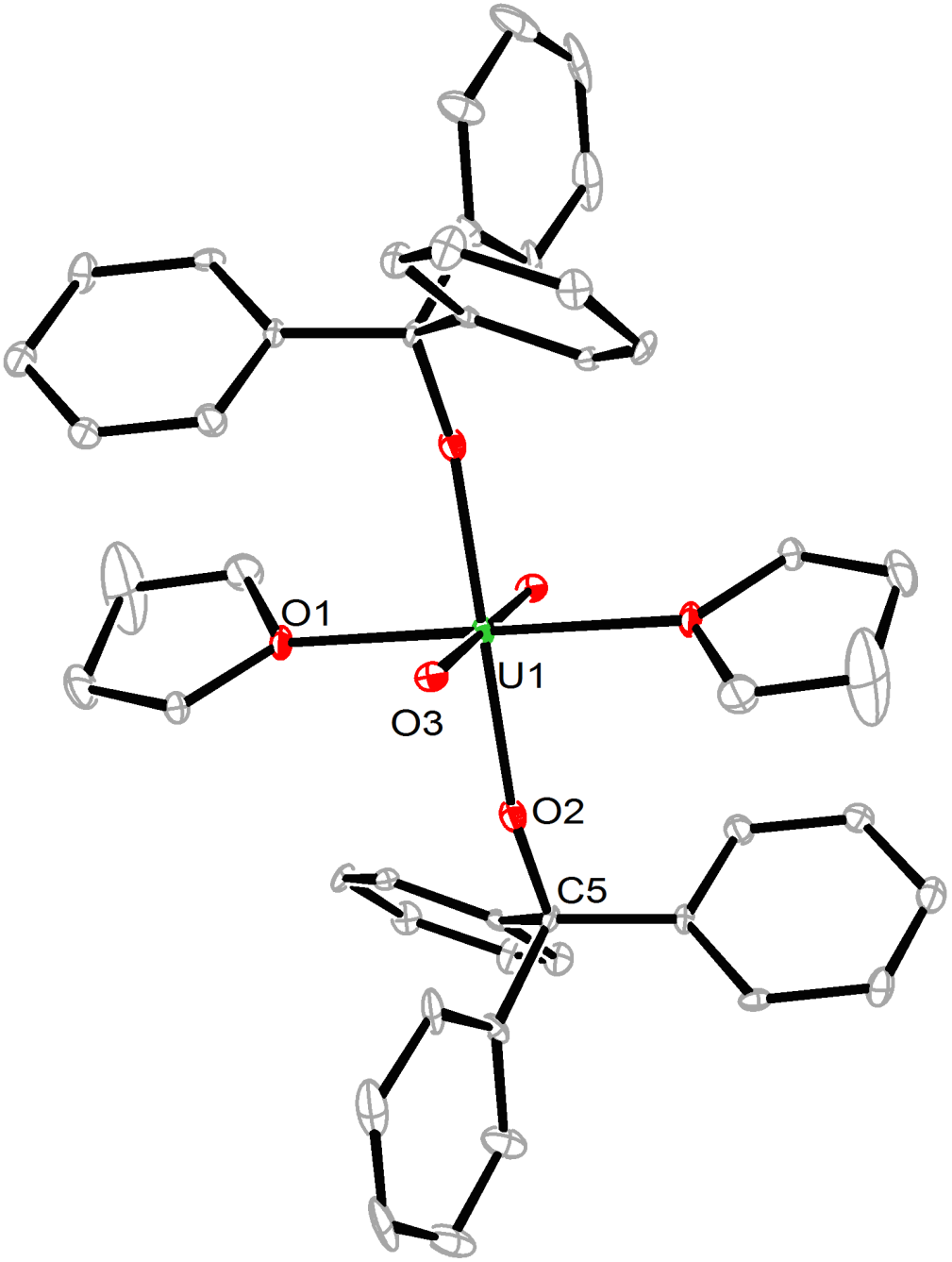

Figure 2.1 ORTEP diagram of $UO_2(OCPh_3)_2THF_2$ **(2.1)** with 20% probability ellipsoids. Selected Bond lengths (Å) and angles (°): U1-O1: 2.414(6), U1-O2: 2.137(6), U1-O3: 1.791(5), O1-C4: 1.444(12), O3-U1-O3*: 180.0, O2-U1-O2*: 180.0, O1-U1-O1*:180.0, U1-O1-C4

The ^{1}H NMR spectrum of complex **2.1** in THF-d_8 exhibits two resonances in the phenyl region at 7.14 ppm and 7.70 ppm, corresponding to the phenyl protons of the alkoxide ligand. In the NMR spectrum there is also residual Et_2O from the reaction. The complex is not completely soluble in THF and will begin to precipitate out of solution after approximately 15 minutes.

2.2.2 Synthesis and Characterization of $UO_2(OCPh_3)_2(THF)(Et_2O)$ (2.2)

The slow diffusion of a diethyl-ether solution of 2 equiv of Ph_3COH into a diethyl ether/hexanes solution of $UO_2[N(SiMe_3)_2]_2(THF)_2$ at -25°C results in the deposition of orange plate like crystals (eq 2.5). X-ray diffraction reveals the structure to be $UO_2(OCPh_3)_2(THF)(Et_2O)$ (**2.2**). Complex **2.2** crystalizes in the triclinic space group P-1 and its solid state structure is shown in Figure 2.2. In the solid state, complex **2.2** exhibits a pseudo-octahedral environment around the uranium center (O5-U1-O6 = 167.9(1)°). The alkoxide ligands are in a cis configuration as opposed to the trans configuration in complex **2.1**. The distortion from an octahedral environment is most likely due to the bulky triphenylmethyl alkoxide ligands being in the cis arrangement. The large steric profile of the triphenylmethyl alkoxide ligands cause a distortion from an octahedral coordination environment and the Et_2O and THF are forced closer to each other to reduce the steric pressure around the alkoxides. This configuration is most likely the less favorable of the two, as evidenced by the reconfiguration to the trans configuration upon being dissolved and recrystallized from THF.

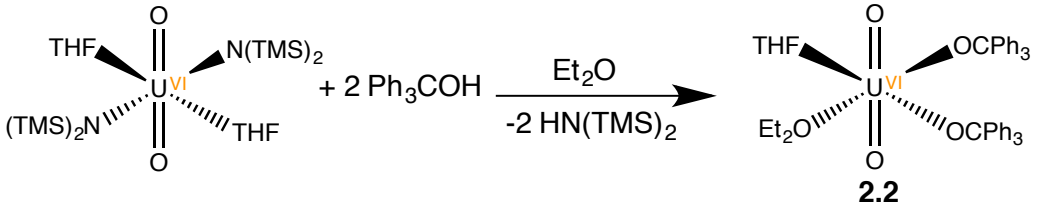

(2.5)

The U-$O_{alkoxide}$ bonds in complex **2.2** are 2.123(3)Å and 2.127(3)Å, which are typical of uranyl alkoxide complexes.[32]

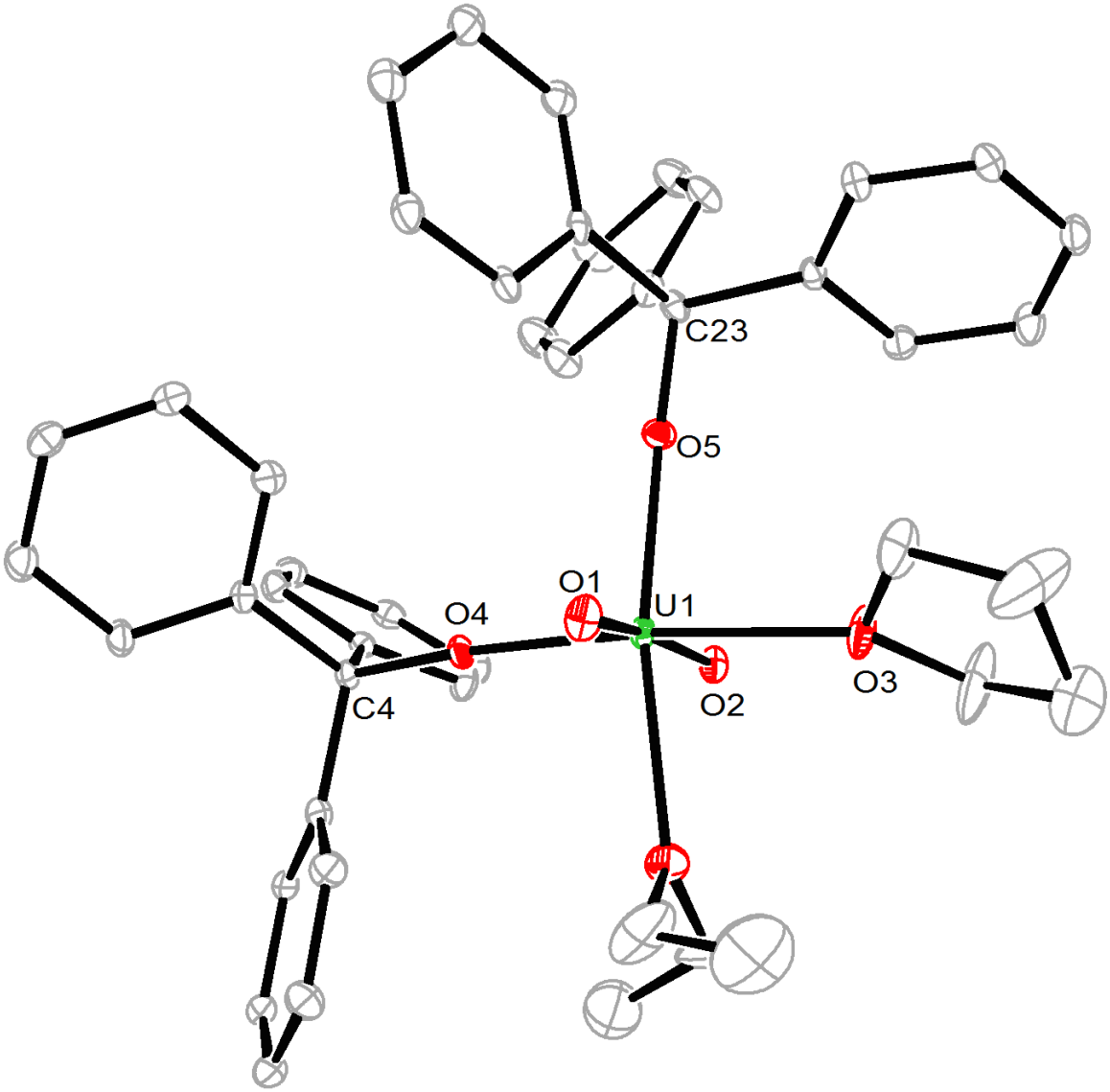

Figure 2.2 ORTEP diagram of $UO_2(OCPh_3)_2(THF)(Et_2O)$ **(2.1)** with 20% probability ellipsoids. Selected Bond lengths (Å) and angles (°): U1-O1: 1.800(4), U1-O2: 1.793(4),

U1-O3: 2.476(4), U1-O4: 2.127(3), U1-O5: 2.123(3), O1-U1-O2: 170.66, O4-U1-O5: 98.1(1), O3-U1-O6: 80.4(2), U1-O4-C4: 174.9(3), U1-O5-C23: 175.2(3)

2.2.3 Reduction of $UO_2(OCPh_3)_2(THF)_2$ (2.1)

The reduction of the complex **2.1** was performed following the procedure utilized by the Hayton group. Upon addition of 4 equiv of KC_8 to the uranyl bis(alkoxide) a deep red color was observed, indicative of the triphenylmethyl anion. The ^{1}H NMR spectrum, in pyridine-d_5, of the reaction mixture only showed the triphenylmethyl anion. Because no uranium containing product could be observed, the reaction was repeated with only 2 equivalents of potassium graphite The solution after filtration had a pale yellow color (eq 2.6) The ^{1}H NMR spectrum of this reaction showed that the product was the previously reported potassium triphenylmethyl alkoxide. This is due to the potassium graphite reducing the uranium center instead of reductively cleaving the ligand as expected. The resulting uranium product would be a uranium IV dioxide which is an insoluble black solid which was filtered away along with the graphite. When 4 equivalents were used, the potassium alkoxide was reduced again forming the triphenylmethyl anion.

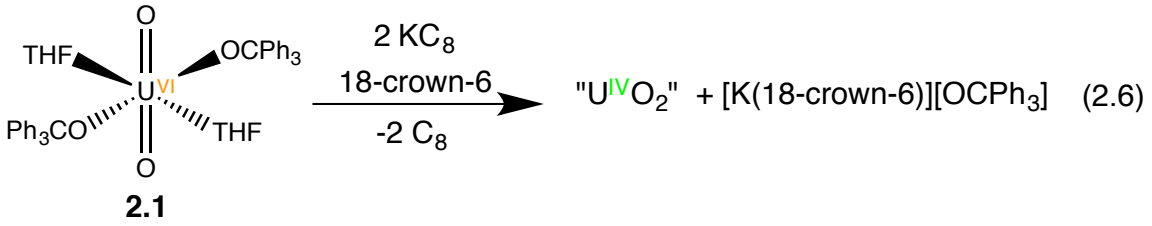

Weaker reducing agents were tested to prevent reducing the metal center. decamethylcobaltocene was utilized. From this reaction, triphenylmethane and Gomberg's dimer, were observed in the ^{1}H NMR spectrum. This is most likely due to the

uranium being reduced and the resulting cobaltacenium alkoxide being unstable due to the lack of direct coordination of the oxygen to a cation. The same reaction was conducted utilizing cobaltocene and there was no reaction.

2.2.4 Synthesis and Characterization of $UO_2(SCPh_3)_2THF_2$ (2.3)

Addition of 2 equivalents of Ph_3CSH to a solution of $UO_2[N(SiMe_3)_2]_2(THF)_2$ in diethyl ether produces an deep red solution from which a brick red precipitate forms. Upon decanting the supernatant, the red solid $UO_2(SCPh_3)2(THF)_2$ (**2.3**) can be isolated in 72% yield (eq 2.7). The red solid is insoluble in alkyl and ethereal solvent and is mildly soluble in pyridine.

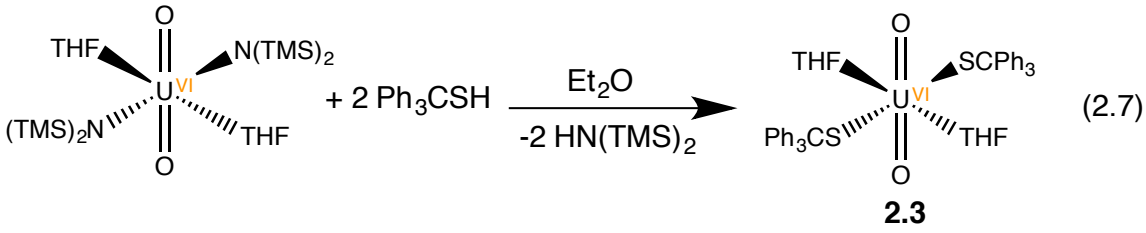

2.3 (2.7)

Single crystals of complex **2.3** were grown by dissolving **2.3** in dichloromethane and diffusing hexanes into the solution at -25 °C. The crystals are red rhomboids and co-deposit with an unidentified beige powder. Complex **2.3** crystallizes in the triclinic space group P-1 and its solid state structure is shown in Figure 2.3. The complex contains a point of symmetry at the uranium center and half of the molecule is grown by symmetry. The U-O_{Uranyl} bond lengths are typical for a uranyl complex at 1.714(13) Å. The U-S bond distance is 2.673(4) Å, which is slightly shorter than the U-S bond distance reported for a similar complex at 2.7325(8) Å.[33] The U-O_{THF} bond distance is 2.39 (1) Å and is typical of uranium –THF distances. The two thiolate ligands are in a trans configuration in the equatorial plane. Due to its poor solubility, and the presence of an unidentified beige decomposition product from dichloromethane, no pure ^{1}H NMR spectrum could be

obtained. The ^{1}H NMR spectrum only shows broad peaks in the phenyl region that could not be assigned.

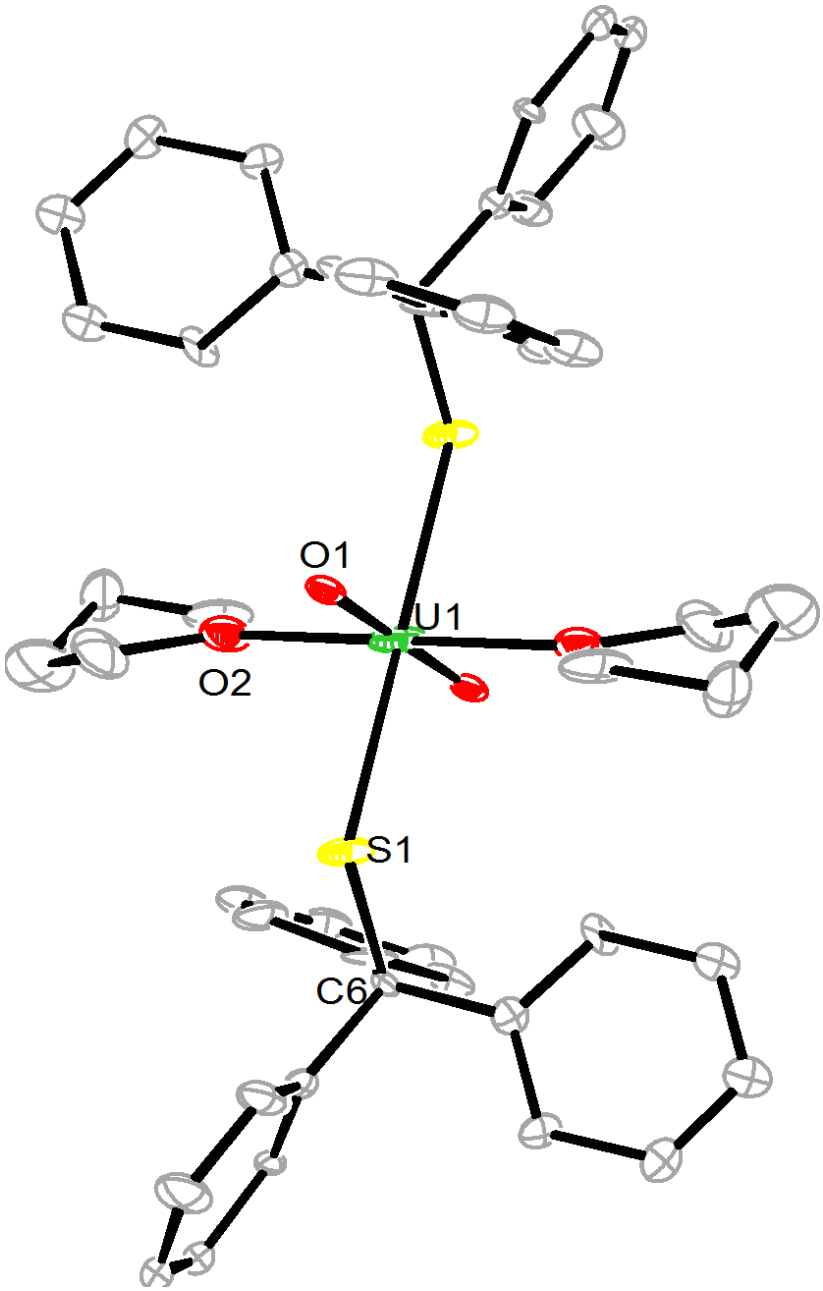

Figure 2.3 ORTEP diagram of $UO_2(SCPh_3)_2THF_2$ **(2.3)** with 20% probability ellipsoids. Selected Bond lengths (Å) and angles (°): U1-O1: 1.714(13), U1-O2: 2.386(15), U1-S1: 2.673(4), S1-C6: 1.872(4), O1-U1-O1*: 180.0, O2-U1-O2*: 180.0, S1-U1-S1:180.0, U1-S1-C6: 121.4(6)

This complex is a rare example of a mononuclear uranyl thiolate complex. The synthesis of uranyl thiolate complexes has been dominated by several bridged species or molecules where the thiolate ligand is a multidentate ligand.[34] There have only been two uranyl thiolate complexes possessing unidentate unsupported ligands reported in the literature and only one was structurally characterized complex. The first structurally characterized uranyl thiolate complex was reported by the Duval group, while the other was reported by the Hayton group. [31,35]

2.2.5 Reduction of $UO_2(SCPh_3)2(THF)_2$ (2.3)

The reduction of complex **2.3** to synthesize a sulfur containing reverse uranyl like structure was performed similarly to that of complex **2.1**. Upon addition of 4 equivalents of potassium graphite to a solution of **2.3** a deep red color formed, indicative of the triphenylmethyl anion. No uranium containing product was observed in the ^{1}H NMR spectrum, only the triphenylmethyl anion. Two equivalents of potassium graphite were reacted with complex **2.3** and potassium thiolate was observed in the ^{1}H NMR spectrum. Similarly to complex **2.1**, the metal center was reduced and $KSCPh_3$ was formed.

Similarly to complex **2.1**, weaker reducing agents were tested to attempt to cleave the carbon-sulfur bond. Two equivalents of decamethylcobaltocene were reacted with complex **2.3** and after approximately 5 minutes red-orange crystals precipitated from the reaction mixture. This complex was decamethylcobaltocenium triphenylmethyl thiolate $[CoCp^*_2][SCPh_3]$(**2.4**) (eq 2.8). Complex **2.4** crystallizes in the monoclinic space group

and its solid state structure is shown in Figure 2.4.

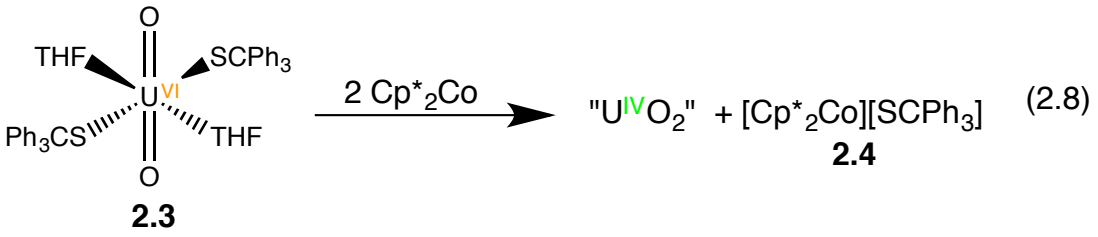

2.3 **2.4** (2.8)

Complex **2.4** crystallizes in the P 21/cspace group as a separated cation anion pair with four of the pairs in the unit cell. The thiolate has a S1-C25 bond distance of 1.85(1) Å, which is typical of a sulfur-carbon bond distance.[36,37] The central carbon C25 has a tetrahedral geometry around it, typical of an sp^3 hybridized carbon. These parameters are typical of thiolate ligands.[38,39] The formation of complex **2.4** indicates that the uranium sulfur bond is weaker than that of the sulfur-carbon bond. The inability to form the desired reverse uranyl like structure and the reduction of the uranium center is indicative of this.

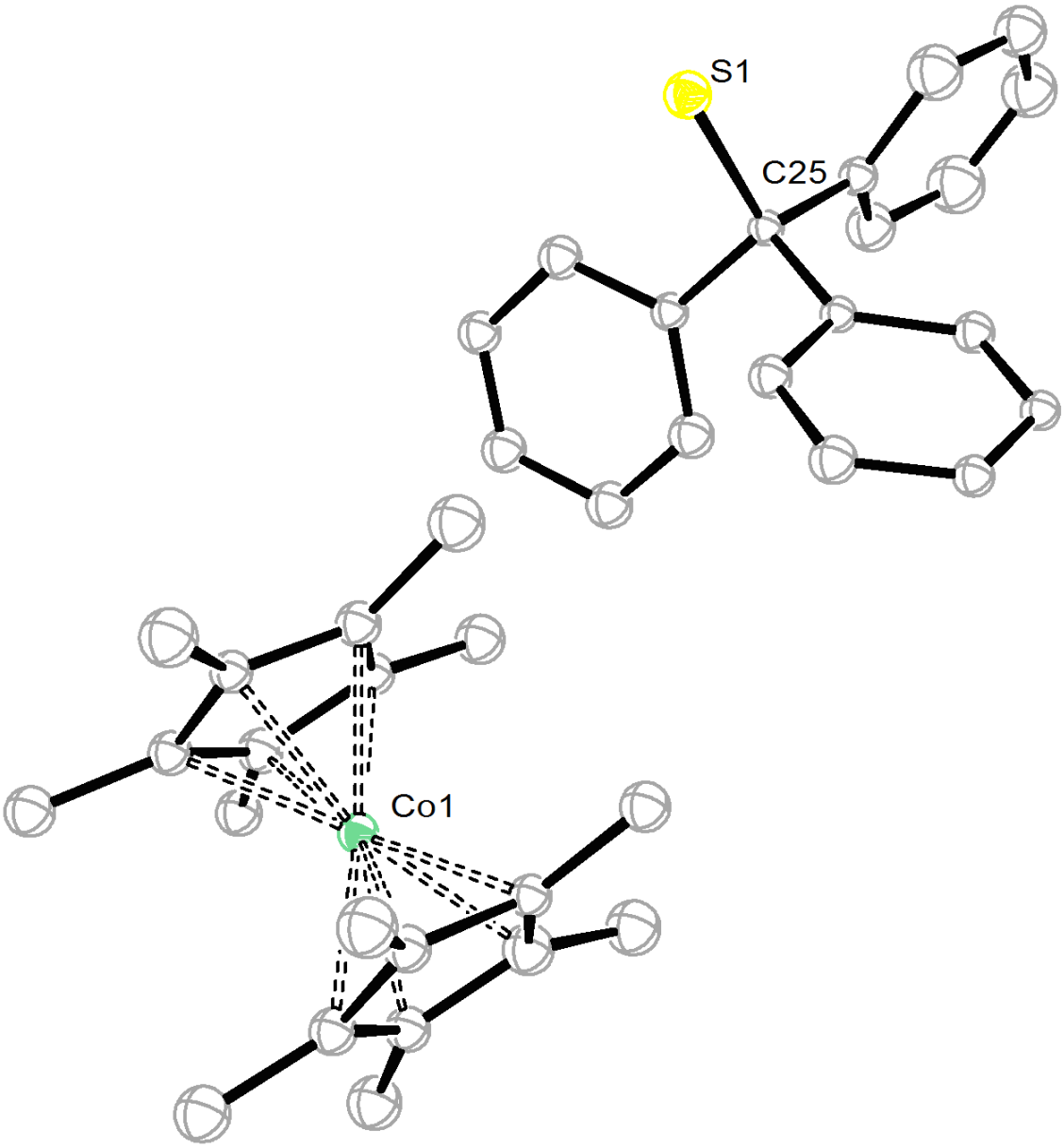

Figure 2.4 ORTEP diagram of $[Cp^*_2Co][SCPh_3]$ (**2.4**) with 20% probability ellipsoids. Selected Bond lengths (Å) and angles (°): S1-C25: 1.85(1); C24-C25; 1.54(1); Co1-C1: 2.06(1); Co1-C3: 2.05(1); Co1-C11:2.042(9); S1-C25-C24:11.9(5); S1-C25-26: 111.6; S1-C25-C32:107.4(7)

2.3 Summary

The isolation of $UO_2(OCPh_3)_2THF_2$ (**2.1**), $UO_2(OCPh_3)_2(THF)(Et_2O)$ (**2.2**), and $UO_2(SCPh_3)_2(THF)_2$ (**2.3**), show that the methodology of utilizing ligand metathesis is a excellent method of synthesizing unsupported alkoxide and thiolate complexes. Uranyl thiolate complexes are extremely rare, and complex **2.3** is only the second unsupported unidentate uranyl thiolate synthesized. Unfortunately, through reactivity studies of these complexes it was found that the reduction of complexes **2.1**, **2.2** and **2.3** does not form the desired reverse uranyl or the sulfur substituted reverse uranyl. The reduction of these complexes reduces the uranium center to uranium(IV), while the ligand is removed from the metal and the free alkoxide or thiolate is formed. The use of potassium graphite resulted in the formation of $KOCPh_3$, $KSCPH_3$ and the utilization of decamethylcobaltacene resulted in the formation of $[CoCp^*_2][SCPh_3]$(**2.4**) while decamethylcobaltacene showed no reactivity with complexes **2.1** and **2.2**. While these complexes did not show the desired reactivity we were able to show that it is easier to reduce off the alkoxide or thiolate ligands and reduce the metal center than to break the oxygen-carbon or sulfur-carbon bonds.

2.4 Experimental

2.4.1 General.

All reactions and subsequent manipulations were performed under anaerobic and anhydrous conditions under an atmosphere of nitrogen. Hexanes, diethyl ether (Et_2O), tetrahydrofuran (THF), and toluene were dried using a Vacuum Atmospheres DRI-SOLV Solvent Purification system and stored over 3Å sieves for 24 h prior to use. Dimethoxyethane (DME) was distilled from sodium benzophenone ketyl and stored over

3Å molecular sieves for 24 h prior to use. Pyridine, benzene-d_6, pyridine-d_5, and tetrahydrofuran-d_8 were dried over 3Å molecular sieves for 24 h prior to use. $UO_2Cl_2(THF)_2$ and $UO_2[N(SiMe_3)_2]_2(THF)_2$ was synthesized according to the previously reported procedures. All other reagents were purchased from commercial suppliers and used as received.

NMR spectra were recorded on a Varian UNITY INOVA 400, a Varian UNITY INOVA 500 spectrometer, or a Varian UNITY INOVA 600 MHz spectrometer. ^1H and $^{13}C\{1H\}$ NMR spectra were referenced to external $SiMe_4$ using the residual protio solvent peaks as internal standards. IR spectra were recorded on a Nicolet 6700 FT-IR spectrometer with a NXR FT Raman Module. UV-Vis / NIR experiments were performed on a UV-3600 Shimadzu spectrophotometer. Elemental analyses were performed by the Micro-Mass Facility at the University of California, Berkeley.

2.4.2 Synthesis of $UO_2(OCPh_3)_2THF_2$ (2.1)

To a stirring solution of $UO_2[N(TMS)_2]_2THF_2$ (0.1394g, 0.190 mmol) in Et_2O (2mL) at room temperature (23 °C), a solution of Ph_3COH (0.0998g, 0.383 mmol) in Et_2O (2mL) was added. The solution immediately turned a bright yellow color and after approximately 30 s, a yellow precipitate formed. The solution was stirred for approximately 10 min then the solid was allowed to settle and the supernatant was decanted. The solid was dried in vacuo then washed with Et_2O (2 x 2mL). The solid was once again dried under vacuum to give 0.1437g (81.2% yield) ^1H NMR (500MHz, 22 °C, THF-d8): 7.14(m 9H, *m*-CH, *p*-CH); 7.70 (*d* 6H, *o*-CH). Anal Calcd for $UO_6C_{46}H_{46}$: C, 59.22; H, 4.97. Found: C, 58.96; H, 5.03.

2.4.3 Synthesis of $UO_2(OCPh_3)_2(THF)(Et_2O)$ (2.2)

To a cold solution (-25°C) of $UO_2[N(TMS)_2]_2THF_2$ (0.0997g, 0.135 mmol) in Et_2O (3mL), hexanes was layered on top (1.5mL). To this solution a cold solution of Ph_3COH (0.0706g, 0.271 mmol) in Et_2O (2mL) was added on top. The solutions were allowed to diffuse together at -25°C for 12h. After 12 h a mixture of orange and yellow crystals were deposited in vial. The orange crystals were the cis product complex **2.2**. The solution was decanted and the solid was dried under vacuum to give 75.3mg (59.5% yield).) ^{1}H NMR (500MHz , 22 °C, THF-d8): 7.14(m 9H, *m*-CH, *p*-CH); 7.70 (d 6H, *o*-CH). Anal Calcd for $UO_6C_{46}H_{46}$: C, 59.22; H, 4.97. Found: C, 58.96; H, 5.03.

2.4.4 Synthesis of $UO_2(SCPh_3)_2THF_2$ (2.3)

To a stirring solution of $UO_2[N(TMS)_2]_2THF_2$ (0.1103g, 0.30 mmol) in Et2O (3mL) at room temperature (22 °C) a solution of Ph_3CSH (.0829g, 0.30 mmol) in Et_2O (2mL) was added. The solution immediately turned a deep red color, and after approximately 30 seconds a brick red precipitate began to form. After stirring for 10min, the solution was decanted and the solid dried under vacuum and 0.1038g was recovered (71.9% yield). Due to the products insolubility, NMR was unable to be performed.

2.4.5 Synthesis of $[Cp^*_2Co][SCPh_3]$ (2.4)

To a slurry of $UO_2(SCPh_3)_2THF_2$ (.0375g, 0.0389 mmol) in THF (2mL) a solution of Cp^*_2Co (0.0256g, 0.0778 mmol) in THF (2mL) was added. After addition and a slight swirling of the vial, the solution turned to a red color. The solution sat still at room temperature (22 °C) for 20 min and red crystals deposited from the solution. The solution was decanted and the crystals were dried under vacuum to give 0.0308g (65.5% yield) ^{1}H NMR (400MHz, 22 °C, pyridine-d_5): 2.22(s, 30H, Cp^*_2Co); 7.10 (m, 3H, *p*-CH); 7.25 (m, 6H, *m*-CH); 8.52 (m, 6H, *o*-CH)

2.4.6 X-Ray Crystallography

Data for complexes **2.1**, **2.2**, **2.3**, and **2.4** were collected on a Bruker KAPPA APEX II diffractometer equipped with an APEX II CCD detector using a TRIUMPH monochromator with a Mo Kα X-ray source (α = 0.71073 Å). The crystals were mounted on a cryoloop under Paratone-N oil, and all data were collected at 100(2) K using an Oxford nitrogen gas cryostream. Data were collected using ω scans with 0.5° frame widths. Frame exposure for complexes **2.1, 2.2** and **2.4** was 5s. The frame exposure for complex **2.3** was 60s. Data collection and cell parameter determination were conducted using the SMART program.[40] Integration of the data frames and final cell parameter refinement were performed using SAINT software.[41] Absorption correction of the data was carried out using the multi-scan method SADABS.[42] Subsequent calculations were carried out using SHELXTL.[43] Structure determination was done using direct or Patterson methods and difference Fourier techniques. All hydrogen atom positions were idealized, and rode on the atom of attachment. Structure solution, refinement, graphics, and creation of publication materials were performed using SHELXTL.[43]

Table 2.1: X-ray Crystallography Data

	2.1	**2.2**	**2.3**	**2.4**
empirical formula	$C_{46}H_{46}O_6U$	$C_{46}H_{48}O_6U$	$C_{46}H_{46}O_4S_2U$	$C_{39}H_{45}O_2SCo$
Crystal habit, color	block, orange	yellow	block, red	block, red
Crystal size (mm)	0.1 × 0.1 × 0.25	0.05 × 0.1 × 0.15	0.1 × 0.1 × 0.2	0.1 × 0.1 × 0.3
Space group	P 21/n	P-1	P-1	P 21/c
volume	1937.0(3)	1985.1(3)	1008.2(10)	3420.8(10)
a (Å)	9.7845(10)	12.9079(10)	8.532(4)	12.733(2)
b (Å)	13.5008(12)	13.1262(10)	10.110(7)	14.658(3)
c(Å)	14.7135(13)	13.9930(11)	13.595(7)	18.407(3)
α (deg)	90	81.601(2)	105.332(14)	90
β (deg)	94.737(4)	63.760(2)	99.212(13)	95.276(5)
γ (deg)	90	69.002(2)	111.503(14)	90
Z	2	2	2	4
formula weight (g/mol)	932.88	934.90	965.01	636.74
density(calculated) (Mg/m^3)	2.001	1.483	1.905	1.236
absorption coefficient (mm^{-1})	8.400	4.133	8.166	0.594
F_{000}	1100	832.0	524	1352
total no. reflections	3971	8235	2900	4298
unique reflections	2766	7430	1608	3619
R_{int}	0.0368	0.0342	0.1003	0.0541
final R indices [I >2σ(I)]	R1= 0.0633 wR2= 0.1657	R1= 0.0399 wR2= 0.1064	R1= 0.1774 wR2= 0.1669	R1=0.0843 wR2=0.2315
largest diff. peak and hole ($e^- A^-$	0.958 to -1.069	1.832 to -1.054	1.625 to -1.730	1.658 and -0.594

^{3})				
GOF	1.166	0.915	1.450	0.962

2.5 References

(1) Brown, J. L.; Fortier, S.; Wu, G.; Kaltsoyannis, N.; Hayton, T. W. *J. Am. Chem. Soc.* **2013**, *135* (14), 5352–5355.

(2) Fortier, S.; Kaltsoyannis, N.; Wu, G.; Hayton, T. W. *J. Am. Chem. Soc.* **2011**, *133* (36), 14224–14227.

(3) Smiles, D. E.; Wu, G.; Hayton, T. W. *Inorg. Chem.* **2014**, *53* (19), 10240–10247.

(4) Tourneux, J.-C.; Berthet, J.-C.; Cantat, T.; Thuéry, P.; Mezailles, N.; Le Floch, P.; Ephritikhine, M. *Organometallics* **2011**, *30* (11), 2957–2971.

(5) King, D. M.; McMaster, J.; Tuna, F.; McInnes, E. J. L.; Lewis, W.; Blake, A. J.; Liddle, S. T. *J. Am. Chem. Soc.* **2014**, *136* (15), 5619–5622.

(6) King, D. M.; Tuna, F.; McInnes, E. J. L.; McMaster, J.; Lewis, W.; Blake, A. J.; Liddle, S. T. *Nature Chem* **2013**, *5* (6), 482–488.

(7) Denning, R. *Struct. Bonding* **1992**, *79*, 215–276.

(8) Denning, R. G. *J. Phys. Chem. A* **2007**, *111* (20), 4125–4143.

(9) Fortier, S.; Wu, G.; Hayton, T. W. *J. Am. Chem. Soc.* **2010**, *132* (20), 6888–6889.

(10) Hayton, T. W.; Boncella, J. M.; Scott, B. L.; Palmer, P. D.; Batista, E. R.; Hay, P. J. *Science* **2005**, *310* (5756), 1941–1943.

(11) Hayton, T. W. *Dalton Trans.* **2010**, *39* (5), 1145–1158.

(12) Kaltsoyannis, N.; Scott, P. *The f elements*; Oxford University Press: New York, 1999.

(13) Tourneux, J.-C.; Berthet, J.-C.; Cantat, T.; Thuéry, P.; Mezailles, N.; Ephritikhine, M. *J. Am. Chem. Soc.* **2011**, *133* (16), 6162–6165.

(14) Anderson, N. H.; Yin, H.; Kiernicki, J. J.; Fanwick, P. E.; Schelter, E. J.; Bart, S. C. *Angew. Chem.-Int. Edit.* **2015**, *54* (32), 9386–9389.

(15) Anderson, N. H.; Odoh, S. O.; Yao, Y.; Williams, U. J.; Schaefer, B. A.; Kiernicki, J. J.; Lewis, A. J.; Goshert, M. D.; Fanwick, P. E.; Schelter, E. J.; Walensky, J. R.; Gagliardi, L.; Bart, S. C. *Nature Chem* **2014**, *6* (10), 919–926.

(16) King, R. B. *Chem. Mater.* **2002**, *14* (9), 3628–3635.

(17) Pyykko, P.; Zhao, Y. *Inorg. Chem.* **1991**, *30* (19), 3787–3788.

(18) Jové, J.; He, L.; Proust, J.; Pagès, M.; Pyykkö, P. *Journal of Alloys and Compounds* **1991**, *177* (2), 285–309.

(19) Pyykko, P.; Zhao, Y. *J. Phys. Chem.* **1990**, *94* (20), 7753–7759.

(20) Bolvin, H.; Wahlgren, U.; Gropen, O.; Marsden, C. *J. Phys. Chem. A* **2001**, *105* (46), 10570–10576.

(21) Smiles, D. E.; Wu, G.; Hayton, T. W. *J. Am. Chem. Soc.* **2014**, *136* (1), 96–99.

(22) Brown, D. R.; Denning, R. G.; Jones, R. H. *Chem. Commun.* **1994**, 2601–2602.

(23) Jones, R. G.; Bindschadler, E.; Blume, D.; Karmas, G.; Martin, G. A., Jr; Thirtle, J. R.; Yeoman, F. A.; Gilman, H. *J. Am. Chem. Soc.* **1956**, *78*, 6030–6032.

(24) Bradley, D. C.; Chatterjee, A. K. *J. Inorg. Nucl. Chem.* **1959**, *12*, 71–78.

(25) Cuellar, E. A.; Miller, S. S.; Marks, T. J.; Weitz, E. *J. Am. Chem. Soc.* **1983**, *105*, 4580–4589.

(26) Bradley, D. C.; Chakravarti, B. N.; Chatterjee, A. K. *J. Inorg. Nucl. Chem.* **1957**, *3* (367), 367–369.

(27) Wilkerson, M. P.; Burns, C. J.; Dewey, H. J.; Martin, J. M.; Morris, D. E.; Paine, R. T.; Scott, B. L. *Inorg. Chem.* **2000**, *39*, 5277–5285.

(28) Burns, C. J.; Smith, D. C.; Sattelberger, A. P.; Gray, H. B. *Inorg. Chem.* **1992**, *31* (18), 3724–3727.

(29) Barnhart, D. M.; Burns, C. J.; Sauer, N. N.; Watkin, J. G. *Inorg. Chem.* **1995**, *34*, 4079–4084.

(30) Schnaars, D. D.; Wu, G.; Hayton, T. W. *J. Am. Chem. Soc.* **2009**, *131* (48), 17532–17533.

(31) Seaman, L. A.; Schnaars, D. D.; Wu, G.; Hayton, T. W. *Dalton Trans.* **2010**, *39* (29), 6635–6637.

(32) Barros, N.; Maynau, D.; Maron, L.; Eisenstein, O.; Zi, G. F.; Andersen, R. A. *Organometallics* **2007**, *26* (20), 5059–5065.

(33) Kannan, S.; Barnes, C. L.; Duval, P. B. *Inorg. Chem.* **2005**, *44*, 9137–9139.

(34) Hayton, T. W. *Chem. Commun.* **2013**, *49* (29), 2956.

(35) Kannan, S.; Barnes, C. L.; Duval, P. B. *Inorg. Chem.* **2005**, *44* (25), 9137–9139.

(36) Smiles, D. E.; Wu, G.; Hayton, T. W. *manuscript in preparation* **2013**.

(37) Rose, D. J.; Chen, Q.; Zubieta, J. *Inorg. Chim. Acta* **1998**, *268*, 163–167.

(38) Holm, R. H. *Acc. Chem. Res.* **1977**, *10* (12), 427–434.

(39) Beardwood, P.; Gibson, J. F. *J. Chem. Soc.-Chem. Commun.* **1986**, *0* (6), 490–492.

(40) 2nd ed. Bruker AXS Inc.: Madison, WI 2005.

(41) 7 ed. Bruker AXS Inc.: Madison, WI 2005.

(42) Sheldrick, G. M. University of Gottingen, Germany 2005.

(43) 6 ed. Bruker AXS Inc.: Madison, WI 2005.

Chapter 3 Experimental Analysis of f-orbital Participation in U-E Multiple Bonds

3.1 Introduction

In the last several years there has been great interest in understanding the amount of covalency in actinide ligand bonds.[1-6] This interest is driven by the potential of using actinide covalent bonding as a means of separating the various metal ions found in nuclear waste.[7,8] Certain lanthanides and actinides have similar ionic radii, such as Am^{3+} and Eu^{3+}, making it difficult to separate these ions relying solely on ionic bonding.[9] The actinides have been shown to exhibit greater covalent bonding than that of the lanthanides and this difference in bonding can be utilized to design new ligands for separating the lanthanides and actinides.[10]

Typically, the bonding of actinide complexes is studied utilizing density functional theory (DFT). DFT enables experimentalists to estimate the individual orbital contributions to the An-L bonds in their synthesized complexes.[11-14] These calculations have been performed on isolated actinide complexes and covalent bonding in these complexes has been studied extensively. [15-22] This approach have been prolific due to its ability to address questions related to the strength and covalency of the uranium heteroatom bonds. Actinide covalency has also been studied experimentally; however, it has only been in recent years that experimental data has been able to address both the strength and covalency of these bonds. Using a myriad of experimental techniques, including ligand K-edge X-ray absorption spectroscopy, EXAFS, and X-ray crystallography, many researchers have been able to quantify actinide ligand covalency in several different systems.[2,3,23,24] Recently Edelstein and co-workers, using NIR spectral data, have been able to quantify actinide covalency in a number of homoleptic octahedral $5f^1$ complexes.[25] Octahedral $5f^1$ complexes were used specifically because of their ability

to address spin-orbit coupling in a relatively straight-forward manner.[25,26] They applied this methodology to uranium halides, alkyls, alkoxides, and ketimides and have been able to quantify the 5f contribution to the uranium-ligand σ and π interactions. This technique relied on the high symmetry of these complexes to extract the θ, Δ, and ξ crystal and ligand field parameters, and from these parameters have been able to quantify the strength and covalency in the actinide ligand bonds in several octahedral complexes. The high symmetry of these complexes results in few transitions in the UV-Vis/NIR spectrum, as shown in figure 3.1, which can be relatively easily assigned.

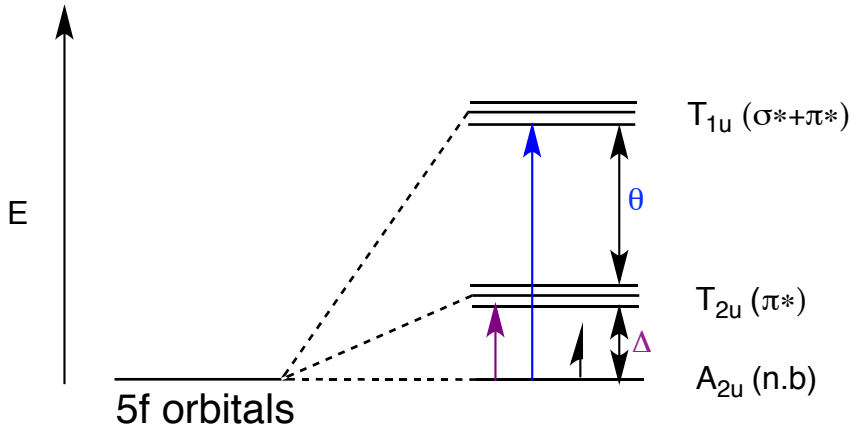

Figure 3.1: f-orbital crystal field splitting in O_h symmetry

Due to the necessity of using homoleptic $5f^1$ complexes with octahedral symmetry, this technique appears to be somewhat limited in scope. However we have hypothesized that it is possible to apply this methodology to certain uranium heteroatom multiple bond systems. Specifically, the ligand field splitting in $5f^1$ systems that contain a multiple bond is dominated by that multiple bonding, with other ligands making minor contributions to the overall bonding motif. With this in mind, we propose that uranium multiply bonded heteroatom complexes in the form $U(E)(NR_2)_3$ (R = $SiMe_3$; E = O, N) can be analyzed as

a $C_{\infty v}$ complex. We hypothesize that $C_{\infty v}$ symmetry is still high enough symmetry that the resulting UV-Vis/NIR spectrum can still be assigned.

The f orbitals of a $C_{\infty v}$ complex are split into a non-bonding Π orbital, a antibonding Δ orbital, an antibonding Π orbital and an antibonding E^+ orbital. As illustrated in figure 3.2, the energy difference between Π and Δ is defined at Δ_1, the energy difference between Δ and Π is defined as Δ_2 and the difference between Π and E^+ is Δ_3. Similar to the octahedral $5f^1$ complexes, the presence of an occupied non-bonding orbital allows for the determination of the absolute strengths of the σ and π interactions between the f orbitals and the ligands.

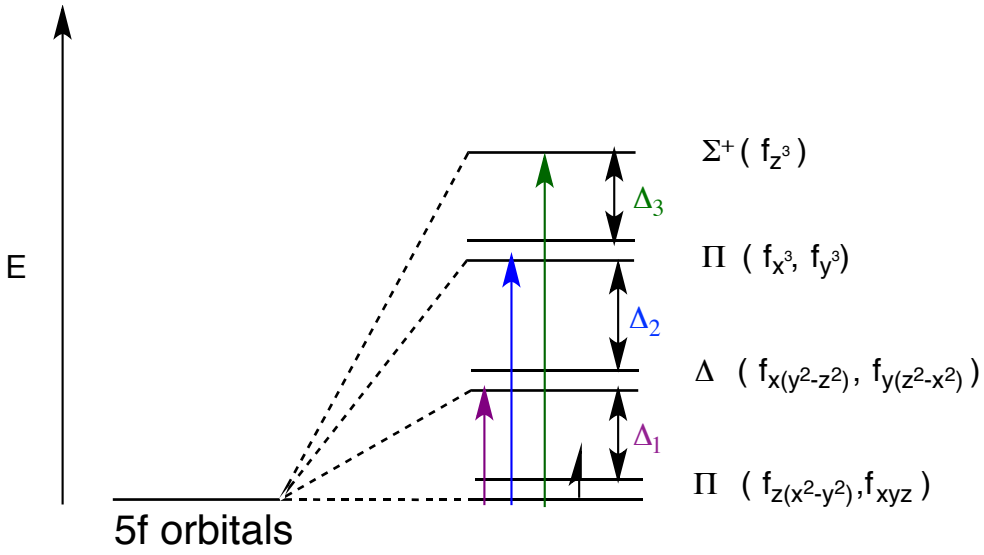

Figure 3.2: f-orbital crystal field splitting in $C_{\infty v}$ symmetry

The expected UV-Vis/NIR spectra for these complexes only take into account the crystal field splitting but not any distortion that occurs due to spin orbit (SO) coupling. In actinide complexes SO coupling is almost as strong as the ligand field.[27] SO coupling mixes the electronic states observed, producing new states. With the octahedral complexes the SO coupling further splits the energy states from three to five. This was

still manageable and the transitions could be assigned. Not accounting for SO coupling we only expect 3 transitions (figure 3.2). Even with SO coupling, the number of transition should still be small. And the assigning the spectrum should still be possible.

3.2 Results and Discussion

3.2.1 Synthesis and Characterization of $(H_{14}C_{10}N)U(NR_2)_3$ (3.1)

Addition of one equivalent of 1-azidoadamantane to $U(NR_2)_3$ (R = $SiMe_3$) in a solution of diethyl ether results in the formation of dark green solution and the evolution of gas. From this solution $(AdN)U(NR_2)_3$ (**3.1**) an be isolated in 70% yield as green needles froma concentrated diethyl ether solution (eq. 3.1).

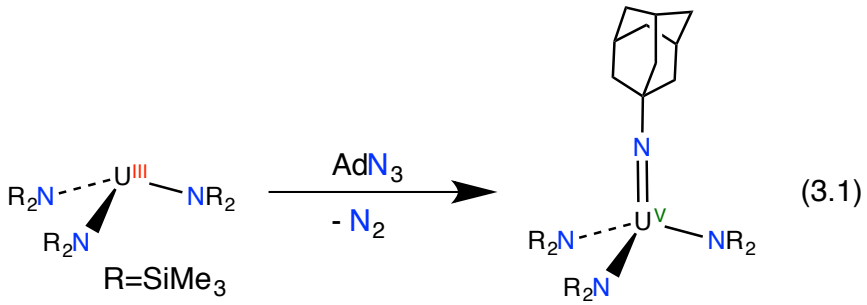

(3.1)

Complex **3.1** is soluble in ethereal solvents. The ^1H NMR spectrum in C_6D_6 exhibits a resonance at -3.90 ppm corresponding to the protons of the NR_2 ligands. It also exhibits resonances at 8.40, 10.47, 16.63 and 19.93 ppm in a 1:1:1:2: ratio corresponding to the four proton environments of the 1-adamantyl imide ligand.

Storage of a concentrated solution of **3.1** in diethyl ether at -25°C results in the formation of crystals suitable for X-ray analysis. Complex **3.1** crystalizes in the trigonal space group P -3 1 c and its solid state molecular structure is shown in Figure 3.3. In the solid state, **3.1** adopts a tetrahedral geometry. The U-N_{amide} bond distances are 2.309(15)

Å, typical of a U(V) amide bond.[28] The U-N imide bond is 2.04(2) Å, similar to other reported uramium imide bond distances.[29-33] The U-N_{Imide}-C bond angle is 180.0° consistent with the multiple bond character of the U-N_{Imide} bond. The N_{amide}-U-N_{imide} bond angle of 110.04(14)° is indicative of the tetrahedral geometry about the uranium center.

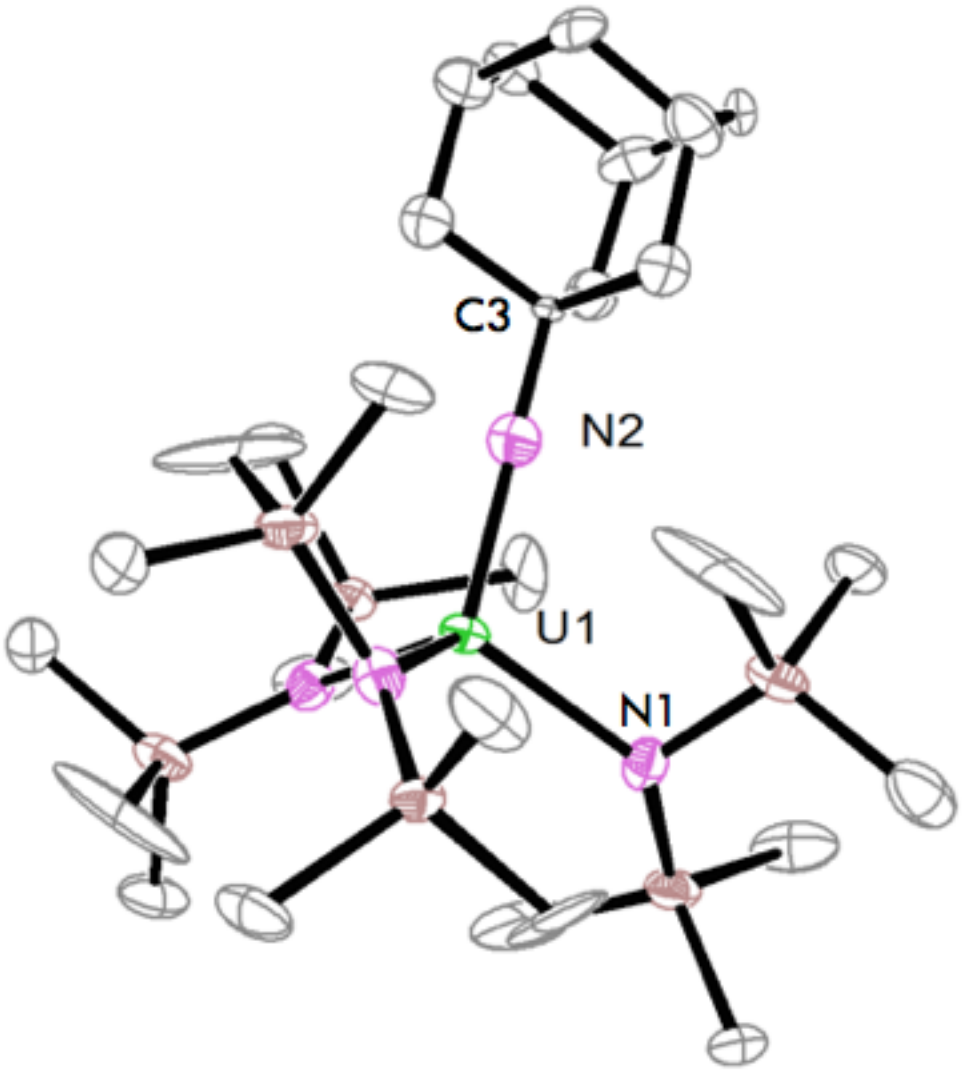

Figure 3.3 ORTEP diagram of $(H_{14}C_{10}N)U(NR_2)_3$ (**3.1**) with 20% probability ellipsoids. Selected Bond lengths (Å) and angles (°): U1-N2: 2.04(2); U1-N1:2.309(15); N2-C3: 1.393(15); N1-U1-N2:110.0(1); N1-U1-N1: 108.9(1)

3.2.2 Electronic Characterization

The characterization of the U^V complexes utilizes data from three characterization methods: UV-Visible/NIR Spectroscopy, Superconducting Quantum Interference Device (SQUID) Magnetometry, and Electron Paramagnetic Resonance (EPR) Spectroscopy. Parameters from these characterization methods are utilized to calculate the f-orbital contribution in the uranium–heteroatom multiple bond. Three complexes were chosen for study using this method: The 1-adamantyl imido complex **3.1**, the previously synthesized trimethylsilyl imido complex $(Me_3SiN)U[NR_2]_3$ **(3.2)**[34] and the previously synthesized oxo complex $(O)U[NR_2]_3$ (**3.3**).[35]

Scheme 3.1: Studied $5f^1$ Complexes

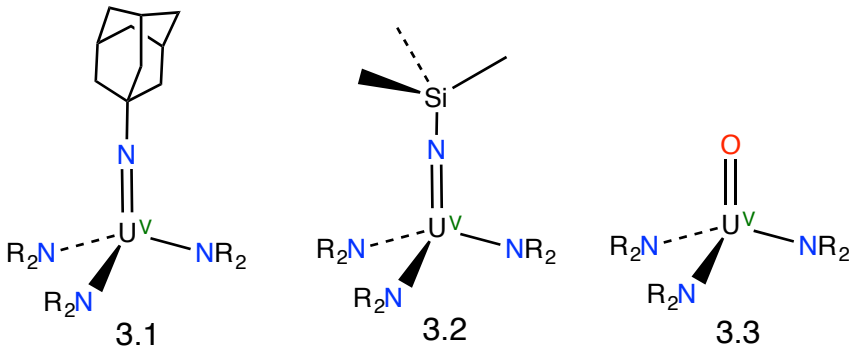

The UV-Visible spectroscopy of complexes **3.1** and **3.2** were performed in deuterated solvents to avoid solvent abosprtions bands overlapping with peaks of the complexes. The spectrum of complex **3.1** (figure 3.4) exhibits three peaks. Based on the predicted electronic configuration of a $5f^1$ complex in $C_{\infty v}$ symmetry, three electronic transitions should be observed. In this spectrum there are indeed three transitions however, in this spectra there may be a fourth transition obscured by the large transition beginning at approximately 1100 nm.

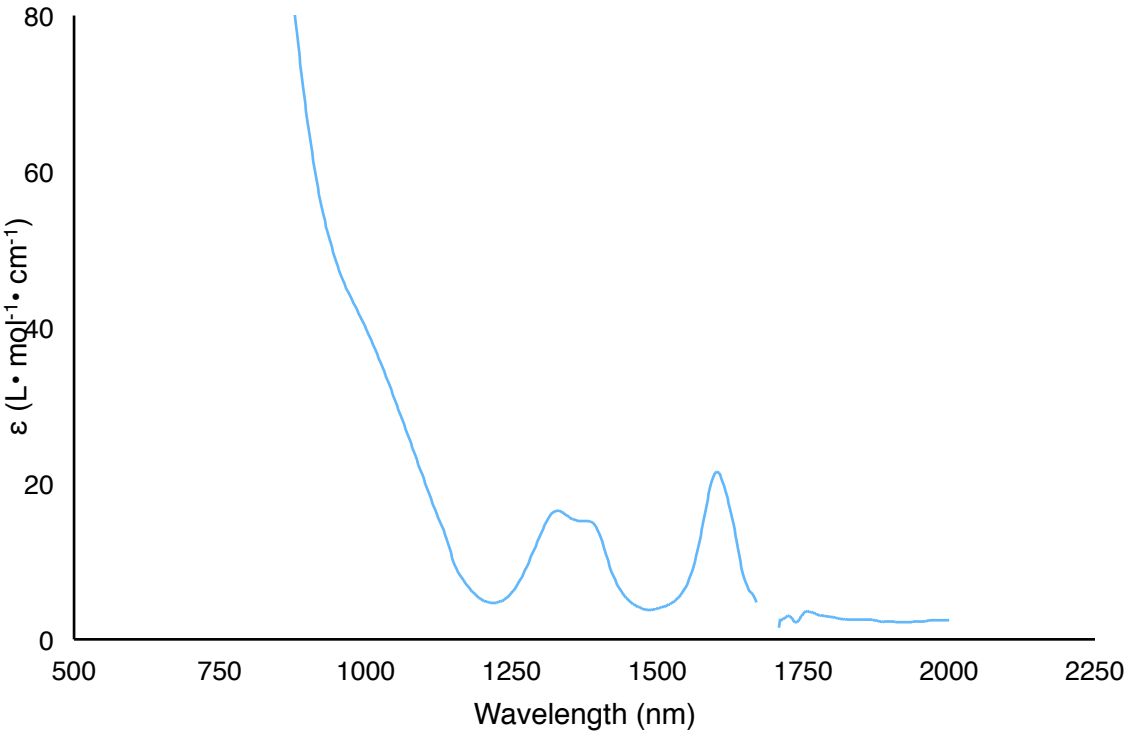

Figure 3.4 Room temperature UV-vis/NIR absorption spectrum for $(H_{14}C_{10}N)U[N(SiMe_3)_2]_3$ **(3.1)** (15.9 mM, C_7H_8).

The UV-Vis/NIR spectrum of complex **3.2** (figure 3.5) contains three peaks similar to the spectra of complex **3.1**. However the peak located at approximately 1100 nm is broad and is most likely representative of multiple overlapping peaks. The extra peaks can be explained due to the fact that the molecular orbital diagram doesn't take into account any spin orbit coupling which may further split the orbital levels. In a previous study done in collaboration with the Hayton group and Dr. Wayne Lukens, several octahedral $5f^1$ complexes were studied.[26] According to the molecular orbital diagram for octahedral $5f^1$ complexes should only have two electronic transitions in its UV-Vis spectrum, however, there are several more due to SO coupling.

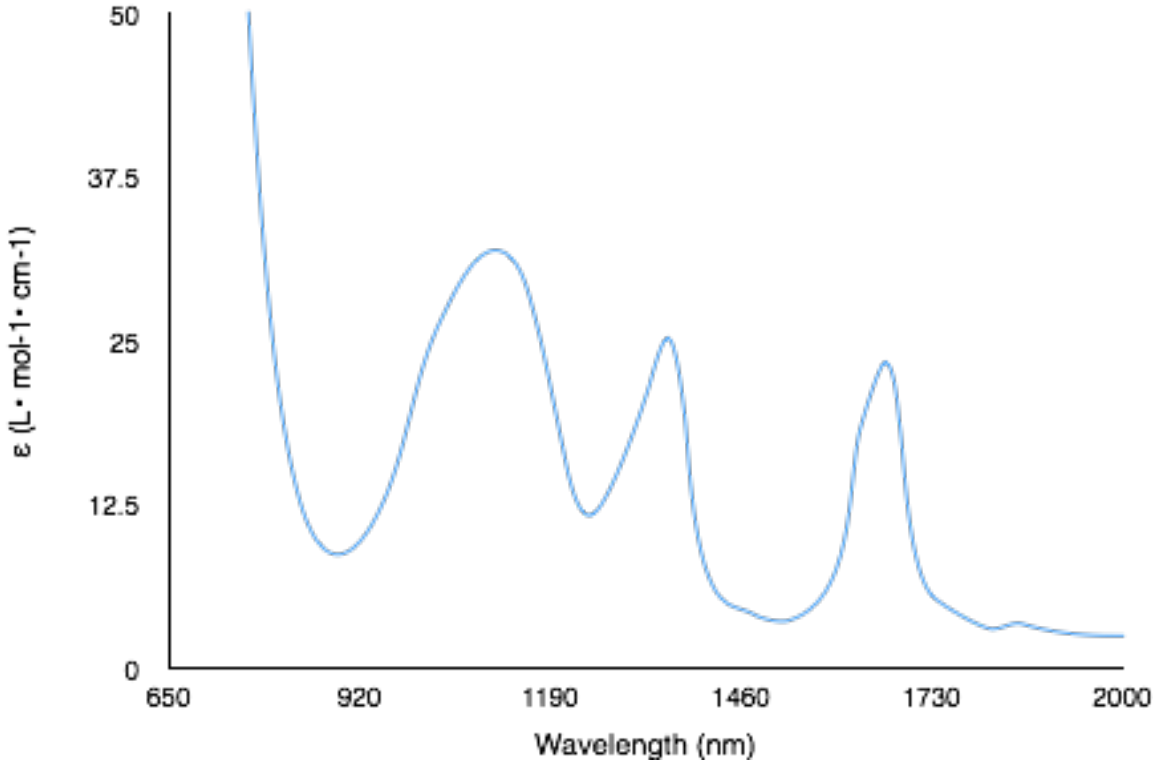

Figure 3.5. Room temperature UV-vis/NIR absorption spectrum for $(Me_3SiN)U[N(SiMe_3)_2]_3$ **(3.2)** (15.66 mM, C_7D_8).

The magnetometry data for complexes **3.1** and **3.2** was also recorded. Complex **3.1** showed an effective magnetic moment of 2.465 μB at 300 K while complex **3.2** showed an effective magnetic moment of 2.119 μB at 300 K (fig 3.6). These values correspond well with the calculated effective magnetic moment of 2.54 μB and correspond well to other reported U(V) complexes.[25,36]

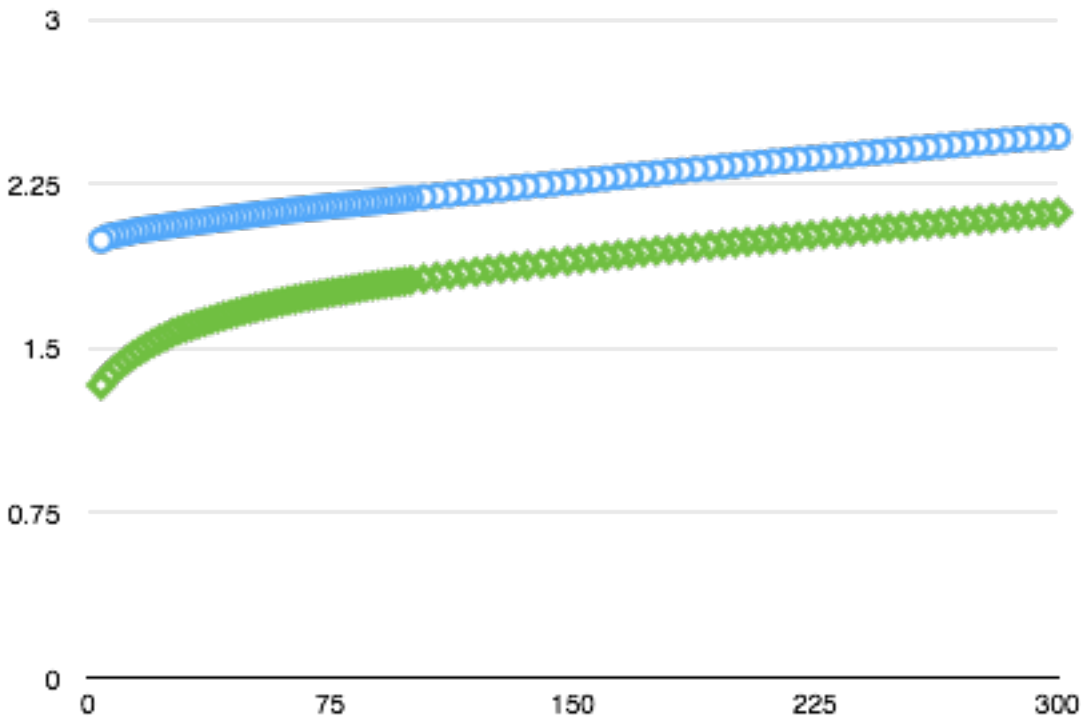

Figure 3.6. Effective magnetic moment of 3.1(O) and 3.2(◆)

3.3 Summary

The understanding of f-orbital interactions in bonding is crucial to the advancement of actinide and lanthanide separation techniques and the management of nuclear waste. The experimental determination of f-orbital participation can be utilized to help understand these interactions better. The expansion of this methodology to new complexes with multiple bonds can show significant increases in f-orbital participation in bonds compared to the previous work. Given the small number of transitions in the UV-Vis spectra, our hypothesis is validated, and it should be possible to complete analysis as intended. With the preliminary data collection completed, calculations are ongoing in collaboration with Lawrence-Berkeley National Lab, which will hopefully show that this methodology does work with non-octahedral complexes.

3.4 Experimental

3.4.1 General

All reactions and subsequent manipulations were performed under anaerobic and anhydrous conditions either under a high vacuum or an atmosphere of argon or nitrogen. Hexanes and diethyl ether (Et_2O) were dried using a Vacuum Atmospheres DRI-SOLV Solvent Purification system and stored over 3Å sieves for 24 h prior to use. All deuterated solvents were purchased from Cambridge Isotope Laboratories Inc. and were dried over activated 3 Å molecular sieves for 24h prior to use. $U[N(SiMe_3)_2]_3$,[37] $(O)U[N(SiMe_3)_2]_3$,[35] $(Me_3SiN)U[N(SiMe_3)_2]_3$, were synthesized according to published procedures. All other reagents were obtained from commercial sources and used as received

NMR spectra were recorded on a Varian UNITY INOVA 400, a Varian UNITY INOVA 500 spectrometer, or a Varian UNITY INOVA 600 MHz spectrometer. ^1H NMR spectra were referenced to external $SiMe_4$ using the residual protio solvent peaks as internal standards. IR spectra were recorded on a Nicolet 6700 FT-IR spectrometer with a NXR FT Raman Module. UV-Vis / NIR experiments were performed on a UV-3600 Shimadzu spectrophotometer.

3.4.2 Synthesis of $(H_{14}C_{10}N)U[N(SiMe_3)_2]_3$ (3.1).

To a stirring solution of $U[N(SiMe_3)_2]_3$ (.4090g, 0.569 mmol in Et_2O (5 mL) was added 1 equiv of 1-azidoadamantane (.1006 g, 0.569 mmol) in Et_2O (1.5 mL). An immediate color change is observed from deep purple to a deep green, along with the evolution of gas from the solution. After stirring for 15 min the solution is reduced in vacuo to 5 mL. Storage of this solution at -25°C for 3 hrs resulted in the deposition of dark green needles (0.3641g, 70%). ^1H NMR (400 MHz, 25 °C, C_6D_6): δ -3.90 (br s,

54H, CH_3), δ 8.40 (s , 3H, CH_2), δ 10.47 (s , 3H, CH_2), δ 16.63 (s , 3H, CH), δ 19.93 (br s , 6H, CH_2). UV−vis−near-IR (C_7H_8,15.9 mM, 25 °C, nm, (L mol^{-1} cm^{-1})): 1040 (sh), 1330 (ε = 16.5), 1382 (ε = 15.2), 1602 (ε = 21.5). IR (KBr pellet, cm−1): 430 (w), 474 (w), 607 (w), 658 (w), 771 (m), 846 (w), 900 (w), 1095(w), 1122 (w), 1179 (w), 1252 (w), 1299 (w), 1365 (w), 1452 (w), 2360 (m), 2851 (w), 2909 (w), 2951 (w).

3.4.3 X-Ray Crystallography

Data for complex **3.1** was collected on a Bruker KAPPA APEX II diffractometer equipped with an APEX II CCD detector using a TRIUMPH monochromator with a Mo Kα X-ray source (α = 0.71073 Å). The crystals were mounted on a cryoloop under Paratone-N oil, and all data were collected at 100(2) K using an Oxford nitrogen gas cryostream. Data were collected using ω scans with 0.5° frame widths. Frame exposure for the complex was 10s. Data collection and cell parameter determination were conducted using the SMART program.[38] Integration of the data frames and final cell parameter refinement were performed using SAINT software.[39] Absorption correction of the data was carried out using the multi-scan method SADABS.[40] Subsequent calculations were carried out using SHELXTL.[41] Structure determination was done using direct or Patterson methods and difference Fourier techniques. All hydrogen atom positions were idealized, and rode on the atom of attachment. Structure solution, refinement, graphics, and creation of publication materials were performed using SHELXTL.[41]

Table 3.1: X-Ray Crystallography Data

	3.1
empirical formula	$C_{12}N_{6.67}Si_{2.33}U$
Crystal habit,	green

color	needle
Crystal size (mm)	0.1 × 0.1 × 0.05
Space group	P -3 1 c
volume	2180.8
a (Å)	14.227(3)
b (Å)	14.227(3)
c(Å)	12.441(3)
α (deg)	90
β (deg)	90
γ (deg)	120
Z	6
formula weight (g/mol)	515.06
density(calculated) (Mg/m^3)	2.353
absorption coefficient (mm^{-1})	11.353
F_{000}	1382
total no. reflections	7533
unique reflections	1503
R_{int}	0.1243
final R indices [I >2σ(I)]	R1=0.1563 wR2=0.30
largest diff. peak and hole ($e^- A^{-3}$)	1.181 to -2.096
GOF	1.384

3.5 References

(1) Neidig, M. L.; Clark, D. L.; Martin, R. L. *Coord. Chem. Rev.* **2013**, *257* (2), 394–406.

(2) Minasian, S. G.; Keith, J. M.; Batista, E. R.; Boland, K. S.; Clark, D. L.; Conradson, S. D.; Kozimor, S. A.; Martin, R. L.; Schwarz, D. E.; Shuh, D. K.; Wagner, G. L.; Wilkerson, M. P.; Wolfsberg, L. E.; Yang, P. *J. Am. Chem. Soc.* **2012**, *134* (12), 5586–5597.

(3) Daly, S. R.; Keith, J. M.; Batista, E. R.; Boland, K. S.; Clark, D. L.; Kozimor, S. A.; Martin, R. L. *J. Am. Chem. Soc.* **2012**, *134* (35), 14408–14422.

(4) Kirker, I.; Kaltsoyannis, N. *Dalton Trans.* **2011**, *40* (1), 124–131.

(5) Schnaars, D. D.; Gaunt, A. J.; Hayton, T. W.; Jones, M. B.; Kirker, I.; Kaltsoyannis, N.; May, I.; Reilly, S. D.; Scott, B. L.; Wu, G. *Inorg. Chem.* **2012**, *51* (15), 8557–8566.

(6) Barros, N.; Maynau, D.; Maron, L.; Eisenstein, O.; Zi, G. F.; Andersen, R. A. *Organometallics* **2007**, *26* (20), 5059–5065.

(7) Morss, L. R.; Edelstein, N. M.; Fuger, J.; Katz, J. J. *The Chemistry of the Actinide and Transactinide Elements*; Springer: Dordrecht, The Netherlands, 2006.

(8) Mazzanti, M.; Weitzke, R.; Pecaut, J.; Latour, J. M.; Maldivi, P.; Remy, M. *Inorg. Chem.* **2002**, *41* (9), 2389–2399.

(9) Shannon, R. D. *Acta Crystallogr. A* **1976**, *A32* (5), 751–767.

(10) Bursten, B. E.; Strittmatter, R. J. *Angew. Chem.-Int. Edit.* **1991**, *30* (9), 1069–1085.

(11) Hohenberg, P.; Kohn, W. *Phys. Rev.* **1964**, *136* (3B), B864–B871.

(12) Kohn, W.; Sham, L. J. *Phys. Rev.* **1965**, *140* (4A), A1133–A1138.

(13) Lee, C.; Yang, W.; Parr, R. G. *Phys. Rev. B* **1988**, *37* (2), 785–789.

(14) Burke, K.; Werschnik, J.; Gross, E. K. U. *The Journal of Chemical Physics* **2005**, *123* (6), 062206.

(15) King, D. M.; Tuna, F.; McInnes, E. J. L.; McMaster, J.; Lewis, W.; Blake, A. J.; Liddle, S. T. *Nat. Chem.* **2013**, *5*, 482–488.

(16) Anderson, N. H.; Odoh, S. O.; Yao, Y.; Williams, U. J.; Schaefer, B. A.; Kiernicki, J. J.; Lewis, A. J.; Goshert, M. D.; Fanwick, P. E.; Schelter, E. J.; Walensky, J. R.; Gagliardi, L.; Bart, S. C. *Nature Chem* **2014**, *6* (10), 919–926.

(17) King, D. M.; McMaster, J.; Tuna, F.; McInnes, E. J. L.; Lewis, W.; Blake, A. J.; Liddle, S. T. *J. Am. Chem. Soc.* **2014**, *136* (15), 5619–5622.

(18) Gardner, B. M.; Balázs, G.; Scheer, M.; Tuna, F.; McInnes, E. J. L.; McMaster, J.; Lewis, W.; Blake, A. J.; Liddle, S. T. *Angew. Chem.-Int. Edit.* **2014**, n/a–n/a.

(19) Gregson, M.; Lu, E.; McMaster, J.; Lewis, W.; Blake, A. J.; Liddle, S. T. *Angew. Chem.-Int. Edit.* **2013**, n/a–n/a.

(20) La Pierre, H. S.; Meyer, K. *Inorg. Chem.* **2013**, *52* (2), 529–539.

(21) Kaltsoyannis, N. *Inorg. Chem.* **2013**, *52*, 3407–3413.

(22) Brown, J. L.; Fortier, S.; Wu, G.; Kaltsoyannis, N.; Hayton, T. W. *J. Am. Chem. Soc.* **2013**, *135* (14), 5352–5355.

(23) Kozimor, S. A.; Yang, P.; Batista, E. R.; Boland, K. S.; Burns, C. J.; Clark, D. L.; Conradson, S. D.; Martin, R. L.; Wilkerson, M. P.; Wolfsberg, L. E. *J. Am. Chem. Soc.* **2009**, *131* (34), 12125–12136.

(24) Daly, S. R.; Keith, J. M.; Batista, E. R.; Boland, K. S.; Kozimor, S. A.; Martin, R. L.; Scott, B. L. *Inorg. Chem.* **2012**, *51* (14), 7551–7560.

(25) Seaman, L. A.; Wu, G.; Edelstein, N. M.; Lukens, W. W.; Magnani, N.; Hayton, T. W. *J. Am. Chem. Soc.* **2012**, *134*, 4931–4940.

(26) Lukens, W. W.; Edelstein, N. M.; Magnani, N.; Hayton, T. W.; Fortier, S.; Seaman, L. A. *J. Am. Chem. Soc.* **2013**, *135* (29), 10742–10754.

(27) Kaltsoyannis, N.; Scott, P. *The f elements*; Oxford University Press: New York, 1999.

(28) Mullane, K. C.; Lewis, A. J.; Yin, H.; Carroll, P. J.; Schelter, E. J. *Inorg. Chem.* **2014**, 140811083351006.

(29) Berthet, J. C.; Thuery, P.; Ephritikhine, M. *Eur. J. Inorg. Chem.* **2008**, No. 35, 5455–5459.

(30) Spencer, L. P.; Yang, P.; Scott, B. L.; Batista, E. R.; Boncella, J. M. *C. R. Chimie* **2010**, *13* (6â€“7), 758–766.

(31) Hayton, T. W.; Boncella, J. M.; Scott, B. L.; Palmer, P. D.; Batista, E. R.; Hay, P. J. *Science* **2005**, *310* (5756), 1941–1943.

(32) Anderson, N. H.; Yin, H.; Kiernicki, J. J.; Fanwick, P. E.; Schelter, E. J.; Bart, S. C. *Angew. Chem.-Int. Edit.* **2015**, *54* (32), 9386–9389.

(33) Schnabel, R. C.; Scott, B. L.; Smith, W. H.; Burns, C. J. *J. Organomet. Chem.* **1999**, *591*, 14–23.

(34) Zalkin, A.; Brennan, J. G.; Andersen, R. A. *Acta Crystallogr. C* **1988**, *44* (9), 1553–1554.

(35) Fortier, S.; Brown, J. L.; Kaltsoyannis, N.; Wu, G.; Hayton, T. W. *Inorg. Chem.* **2012**, *51* (3), 1625–1633.

(36) Spencer, L. P.; Schelter, E. J.; Yang, P.; Gdula, R. L.; Scott, B. L.; Thompson, J. D.; Kiplinger, J. L.; Batista, E. R.; Boncella, J. M. *Angew. Chem.-Int. Edit.* **2009**, *121* (21), 3853–3856.

(37) Anderson, R. A. *Inorg. Chem.* **1979**, *18* (1), 209.

(38) 2nd ed. Bruker AXS Inc.: Madison, WI 2005.

(39) 7 ed. Bruker AXS Inc.: Madison, WI 2005.

(40) Sheldrick, G. M. University of Gottingen, Germany 2005.

(41) 6 ed. Bruker AXS Inc.: Madison, WI 2005.

Chapter 4 Exploration of the Synthesis of Uranium Pnictogen Multiple Bonds: New Pathways to Phosphorus Atom Transfer

4.1 Introduction

The separation of lanthanides from the actinides has been a subject of study for several decades.[1-7] The lanthanides and actinides are both present in nuclear waste and the late actinides created during fission account for majority of the radioactivity of nuclear waste. If the lanthanides are removed the amount of radioactive waste needed to be stored could be reduced. However, it has proven quite difficult to separate the lanthanides and actinides. The ionic radii of several of the lanthanides and actinides are too similar, such as Am, Cm, Nd, and Pm, and it is extremely difficult to separate them on the basis of their ionic radii.[8] The actinides and lanthanides also have similar ionic charges so their ionic properties can't be used for separation either. Several studies have been done utilizing several different chemical separation ligands to test the effectiveness of different ligands.[7,9] It was found that when using tributylphosphate (TBP) there was no separation between americium and europium. However, once the ligand was changed to a thiophosphinic acid, Cyanex-301, there was greater selectivity for americium and a separation factor of 3200. [7,9]

Scheme 4.1: Actinide Extraction Agents

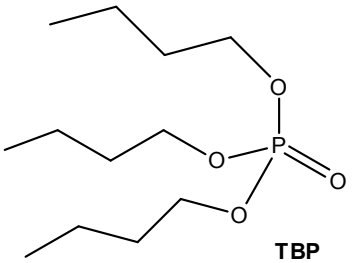

TBP

$S_{\frac{Am}{Eu}}$

1.0

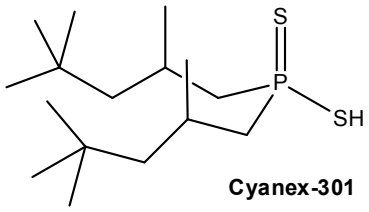

Cyanex-301

3200

It was proposed that the cause of this difference in selectivity was the actinides being able to covalently interact with the softer donor sulfur atoms. The 5f orbitals in the actinides are less shielded than the 4f orbitals in the lanthanides and are more available for bonding.[10] The bonding of the lanthanides is more ionic in nature and the ability of the actinides to perform covalent bonding can prove to be useful for separating actinides and lanthanides.

To study covalency in the actinides, uranyl complexes were studied to observe the participation of 5f orbitals in the uranium-oxygen multiple bonds.[11-16] The study of these complexes has shown significant f-orbital participation in the oxo bonds. To increase the knowledge about f-orbitals several uranyl analogues were synthesized replacing the hard donor oxygen with heavier, softer donor chalcogens.[17] These complexes also showed significant covalency in the multiple bonds in the DFT calculations. Several of complexes containing actinide-chalcogen multiple bonds have been synthesized and studied, including the recent synthesis of a full series of terminal chalcogenides

synthesized by the Hayton group.[18,19] These complexes have provided good insight into how the 5f orbitals interact with these elements, however, just the chalcogens alone are not enough. The next step in this work was to expand to the pnictogens to see how the f-orbitals interact with more donor atoms.

The study of actinide pnictogen bonding has been ongoing and amides have frequently been used as co-ligands for many metal complexes.[20] The expansion to actinide pnictogen multiple bonds however are relatively recent. The synthesis of uranium imido complexes began in 1980's when Gilje and coworkers synthesized the first actinide imido complex $Cp_3UNC(Me)CHP(Ph)_2Me$.[21] Several other uranium imido complexes have been synthesized and studied in the past several decades and have exhibited a fair amount of covalency and f-orbital participation. This research expanded into making an imido analogue of uranyl, which was synthesized by Boncella and co-workers in 2005. [22-24] The exploration of pnictogen multiple bonds have expanded to nitride complexes in recent year. The Hayton group recently published the synthesis of a bridged uranium nitride complex.[25] This bridging nitride was then used to synthesize an oxy-nitrido complex, a nitride substituted analogue of uranyl. In 2013, Liddle and co-workers reported the synthesis of a terminal uranium nitride complex. [26,27] The expansion of actinide pnictogen chemistry has led us to explore new uranium-nitrogen multiply bonded complexes and also expand this chemistry to the rest of the pnictogens.

Metal-phosphorus multiple bonding has also been explored for several decades.[28,29] Phosphinidenes have been synthesized for several decades and there are over 130 structurally characterized phosphinidenes in the literature. Several uranium phosphinidene complexes have been synthesized previously. Marks and coworkers

reported the synthesis of a bridging phosphinidene complex in 1984, and Burns and coworkers reported the synthesis of a terminal uranium phosphinidene in 1996.[30,31]

Scheme 4.2: Uranium Phosphinidenes

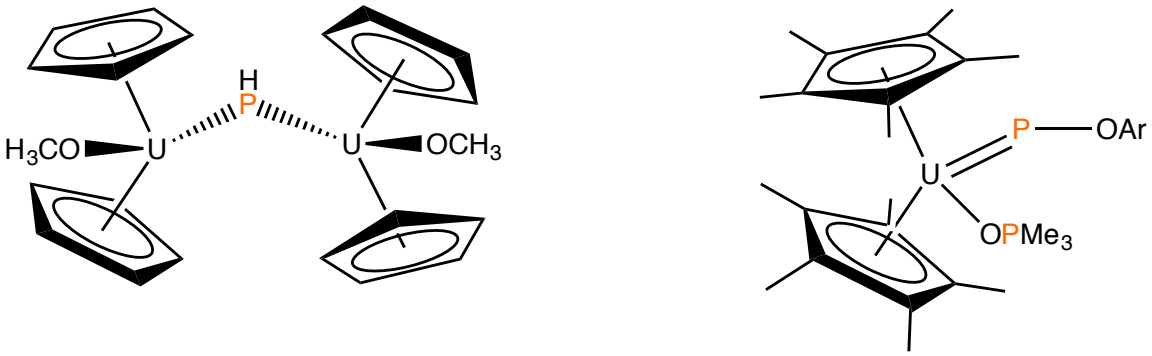

Phosphide chemistry is less explored than phosphinidenes, and only approximately 20 phosphides have been structurally characterized. The first metal phosphides were synthesized in 1995 by Schrock and coworkers, with the synthesis of tungsten and molybdenum phosphides.[32] Several other group 6 metal phosphides have been synthesized along with two niobium nitride complexes.[33-36] Recently the Liddle group synthesized a terminal uranium phosphide and it was found that the uranium contribution to the bond had significant f-orbital character.[37] The growth of f-orbital pnictogen chemistry has inspired us to look for new uranium pnictogen bonding methods and synthesize new complexes.

4.2 Results and Discussion

4.2.1 Synthesis and Characterization of [Na(18-crown-6)][(N(SiMe$_3$)$_2$)$_2$U(μ-N)(*Se*CH$_2$SiMe$_2$*N*(SiMe$_3$))U(N(SiMe$_3$)$_2$)$_2$](4.1)

Following the success of the formation of the oxy-nitrido, the synthesis of the analogous selenide and telluride complexes were attempted. Upon reacting the [Na(DME)$_3$][(N(SiMe$_3$)$_2$)$_2$U(μ-N)(CH$_2$SiMe$_2$*N*(SiMe$_3$))U(N(SiMe$_3$)$_2$)$_2$] with 1 equiv of

elemental selenium, in diethyl ether, in the presence of 18-crown-6, dark brown crystals were isolated from the dark brown reaction mixture upon workup. An X-ray crystallographic analysis showed that this complex was not the intended terminal selenide, but in fact a selenium-bridged U^{IV}/U^{IV} bimetallic metallacycle complex (eq 4.1). The complex [Na(18-crown-6)][$(N(SiMe_3)_2)_2U(\mu$-N)(*Se*CH_2SiMe_2*N*$(SiMe_3)$)U$(N(SiMe_3)_2)_2$] (**4.1**) (eq 4.1) was isolated in 42% yield, which can be improved to 54% via treatment of [$Na(DME)_3$][$(N(SiMe_3)_2)_2U(\mu$-N)(CH_2SiMe_2*N*$(SiMe_3)$)U$(N(SiMe_3)_2)_2$] with 1 equiv Ph_3PSe.

The room temperature ^{1}H NMR spectrum of **4.1** in *d5*-pyridine exhibits 6 resonances at -41.83, -24.03, -5.55, 18.47, 22.85 and 50.41 in a 2:2:2:2:1:1 ratio, respectively. This ratio of resonances was unexpected. The expected resonances should be in a 36:36:9:6:2 ration, but that is not observed. Variable temperature experiments are needed to fully assign the spectrum.

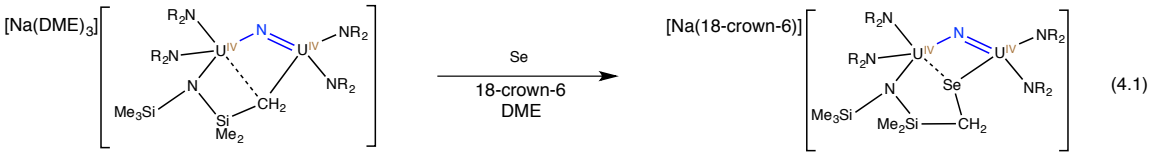

(4.1)

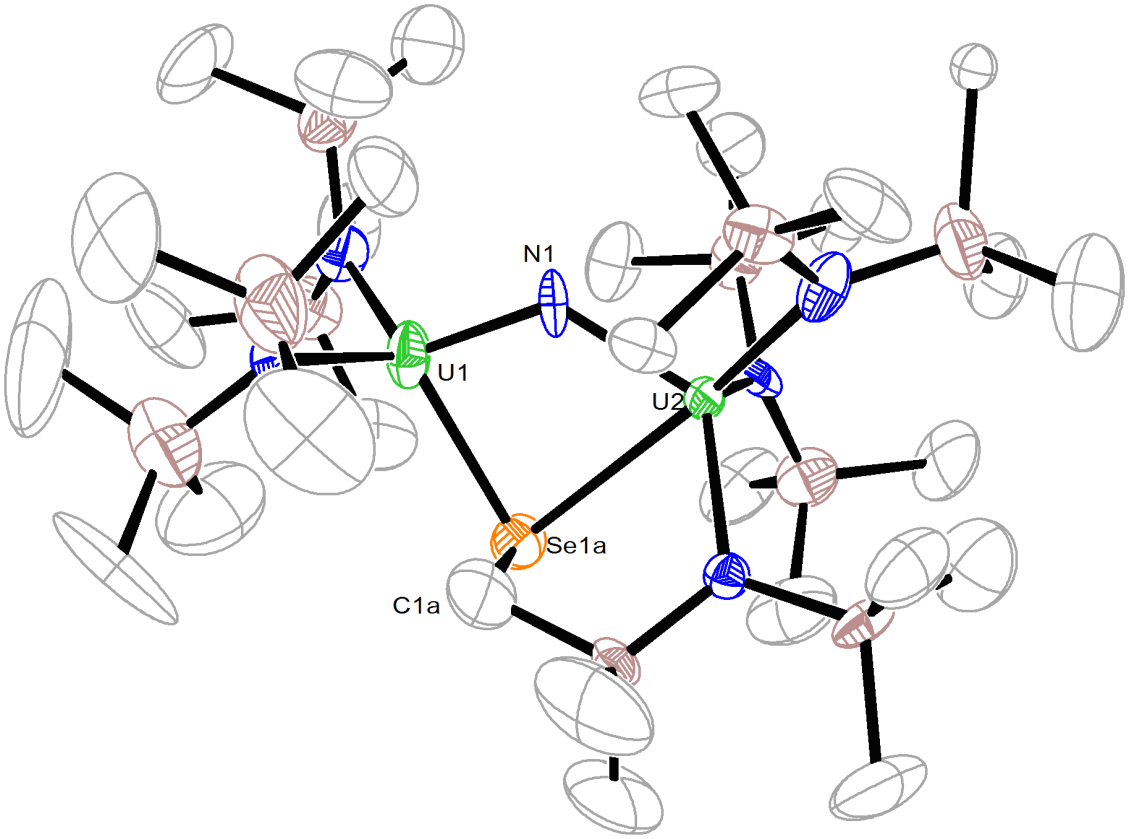

Figure 4.1 ORTEP diagram of [Na(18-crown-6)][(N(SiMe$_3$)$_2$)$_2$U(μ-N)(*Se*CH$_2$SiMe$_2$*N*(SiMe$_3$))U(N(SiMe$_3$)$_2$)$_2$] (**4.1**) with 20% probability ellipsoids. Na(18-crown-6) omitted for clarity. Selected Bond lengths (Å) and angles (°): U1-N1: 1.959(17); U2-N1: 2.15(1); U1-Se1A: 2.762; U2-Se1A: 3.113(4); Se1A-C1a: 2.24(7); U1-N1-U2: 126.1(1)

Complex **4.1** crystallizes in the triclinic space group P-1, with two independent molecules in the unit cell. Complex **4.1** displays U-N$_{nitride}$ bond distances of U1-N1 = 1.96(1) Å and U2-N1 = 2.15(1) Å, a slight elongation compared to [Na(DME)$_3$][(N(SiMe$_3$)$_2$)$_2$U(μ-N)(CH$_2$SiMe$_2$*N*(SiMe$_3$))U(N(SiMe$_3$)$_2$)$_2$]. This is likely due to the increased U-N-U bond angle of 126.1(10)°, due to the increased length of the

U-Se interaction in comparison to the U-CH_2 interactions in $[Na(DME)_3][(N(SiMe_3)_2)_2U(\mu\text{-}N)(CH_2SiMe_2\mathit{N}(SiMe_3))U(N(SiMe_3)_2)_2]$**.** The solid-state molecular structure of **4.1** displays U-Se bond distances of U1-Se =2.762(5) Å and U2-Se =3.113Å. These inequivalent U-Se interactions are reminiscent of the U-CH_2 interactions $[Na(DME)_3][(N(SiMe_3)_2)_2U(\mu\text{-}N)(CH_2SiMe_2\mathit{N}(SiMe_3))U(N(SiMe_3)_2)_2]$ The U1-Se bond distance and the Se-C1 bond distance of 2.24(7) Å are typical of a U-Se and Se-C single bonds.[19]

4.2.2 Synthesis and characterization of $[Na(18\text{-crown-}6)][(N(SiMe_3)_2)_2U(\mu\text{-}N)(\mathit{Te}CH_2SiMe_2\mathit{N}(SiMe_3))U(N(SiMe_3)_2)_2]$ (4.2)

In an effort to synthesize the analogous tellurium complex, the addition of elemental Te to $[Na(DME)_3][(N(SiMe_3)_2)_2U(\mu\text{-}N)(CH_2SiMe_2\mathit{N}(SiMe_3))U(N(SiMe_3)_2)_2]$ was carried out in the presence of 18-crown-6 and triethylphosphine (eq 4.3). Dark brown crystals were isolated and X-ray crystallographic analysis showed the complex $[Na(18\text{-crown-}6)][(N(SiMe_3)_2)_2U(\mu\text{-}N)(\mathit{Te}CH_2SiMe_2\mathit{N}(SiMe_3))U(N(SiMe_3)_2)_2]$ (**4.2**), an inserted telluride, isostructural to complex **4.1**.Complex 4.2 can be isolated in 59% yield.

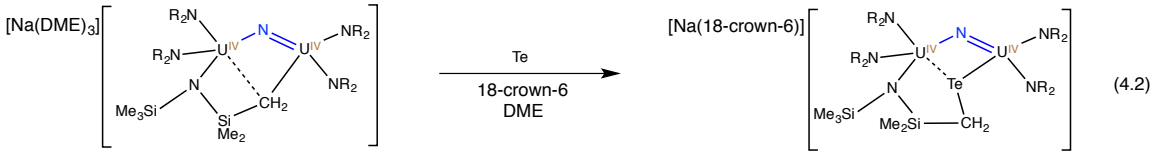

(4.2)

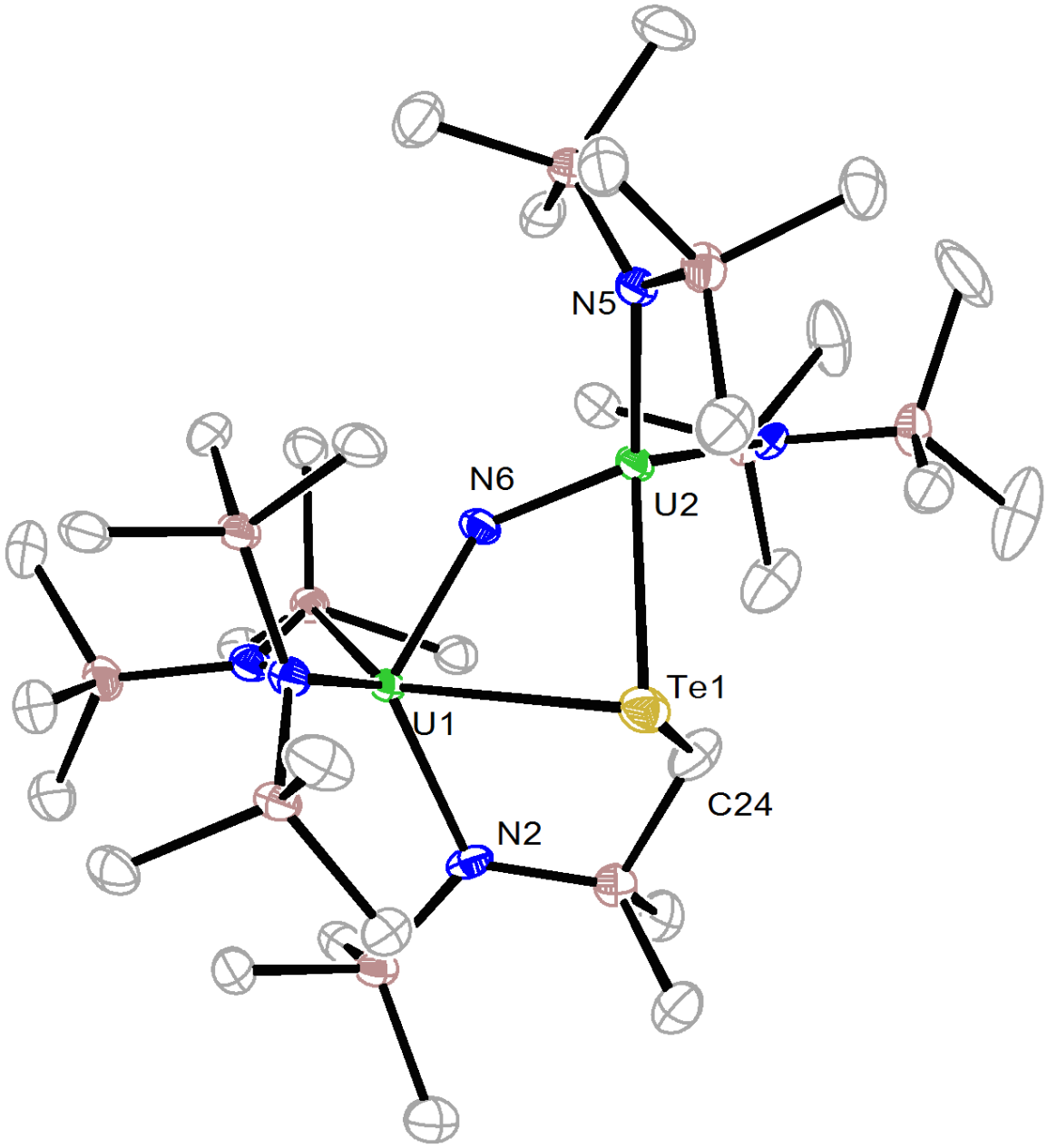

Figure 4.2 ORTEP diagram of [Na(18-crown-6)][(N(SiMe$_3$)$_2$)$_2$U(μ-N)(*Te*CH$_2$SiMe$_2$*N*(SiMe$_3$))U(N(SiMe$_3$)$_2$)$_2$] (**4.2**) with 20% probability ellipsoids. Na(18-crown-6) omitted for clarity. Selected bond lengths (Å) and angles (°): U1-N6: 2.118(5); U2 N6: 2.000(4); U1-Te1: 3.3284(5); U2-Te1: 3.06(1); Te1-C24: 2.184(6); U1-N6-U2: 132.5(3)

The room temperature ^{1}H NMR spectrum of **4.2** in *d5*-pyridine exhibits 6 resonances at -114.90, -40.06, -24.7-, -3.06, 18.64, and 49.85 ppm. Complex **4.2** also crystallizes in the triclinic space group P-1, with the unit cell containing two independent molecules. The U-$N_{nitride}$ bonds are further elongated, U1-N6= 2.000(4) Å and U2-N6 = 2.118(5) Å, while the U-N-U bond angle also experiences an increase (132.5(3)°). The increase in the U-N-U angle can be explained by the increased radius of tellurium versus selenium.

4.2.3 Synthesis of [Na(18-crown-6)][$(N(SiMe_3)_2)_2(C_{10}H_{15}N)U(\mu$-N)($CH_2SiMe_2$*N*($SiMe_3$))U($N(SiMe_3)_2)_2$] (4.3)

In an effort to further explore the reactivity of[$Na(DME)_3$][$(N(SiMe_3)_2)_2U(\mu$-N)(CH_2SiMe_2*N*($SiMe_3$))U($N(SiMe_3)_2)_2$] with oxidizing agents, reactivity with organic azides was explored. Organic azides have long been shown to be excellent precursors to imidos.[38]

Upon addition of 1-azidoadamantane to [$Na(DME)_3$][$(N(SiMe_3)_2)_2U(\mu$-N)(CH_2SiMe_2*N*($SiMe_3$))U($N(SiMe_3)_2)_2$] an evolution of gas occurred and the solution changed to a dichroic red-green. From this reaction mixture deep red green crystals were isolated. Analysis with X-ray crystallography showed this to be [$Na(DME)_3$][$(N(SiMe_3)_2)_2(C_{10}H_{15}N)U(\mu$-N)($CH_2SiMe_2$*N*($SiMe_3$))U($N(SiMe_3)_2)_2$] (**4.3**). Complex **4.3** crystallizes in the monoclinic space group P2(1)/c and contains four independent molecules in the unit cell.

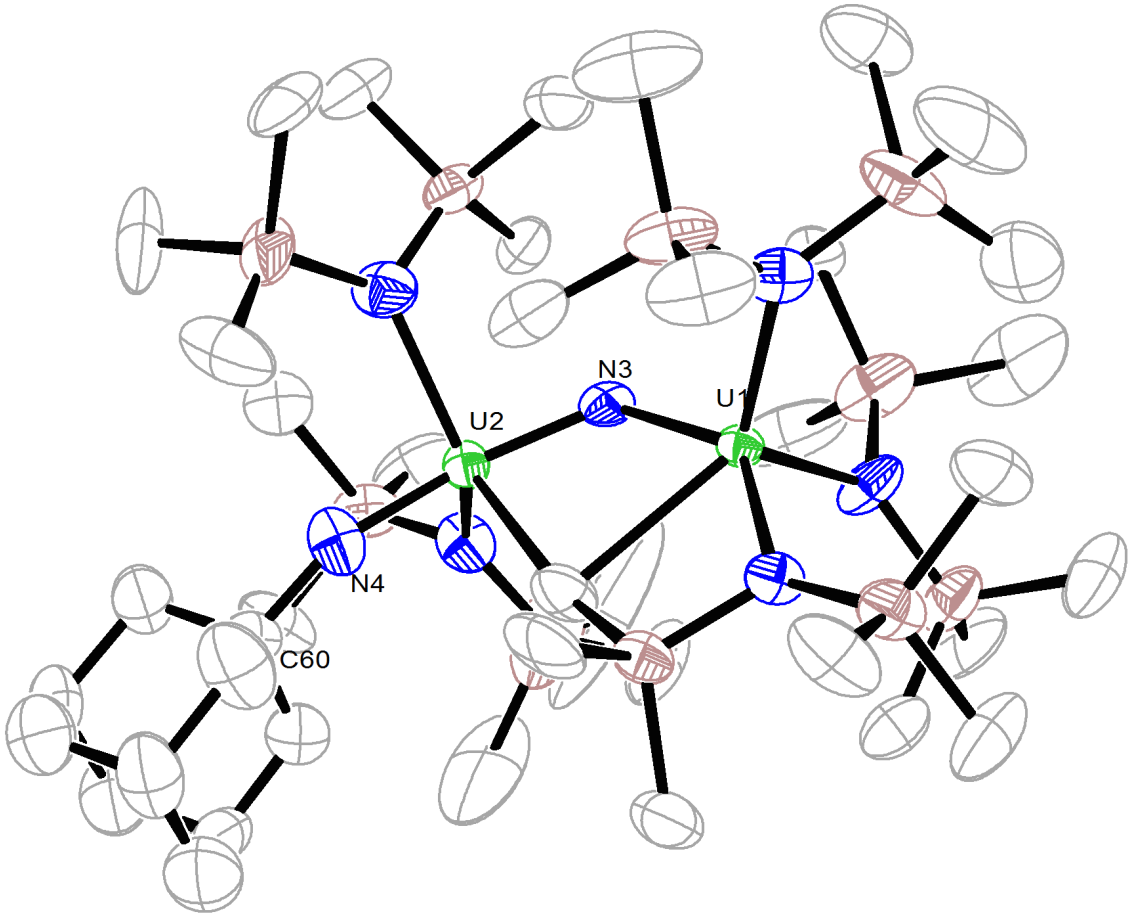

Figure 4.3 ORTEP diagram of [Na(18-crown-6)][(N(SiMe$_3$)$_2$)$_2$(C$_{10}$H$_{15}$N)U(μ-N)(CH$_2$SiMe$_2$*N*(SiMe$_3$))U(N(SiMe$_3$)$_2$)$_2$](**4.3**) with 20% probability ellipsoids. Na(18-crown-6) omitted for clarity. Selected bond lengths (Å) and angles (°): U1-N3: 2.257(11); U2-N3:1.857(11); U2-N4:1.851(11); U1-C14:2.674(14); N4-C60: 1.1537(17); U1-N3-U2: 123.0(5);N3-U2-N4: 163.0(5)

The room temperature ^{1}H NMR spectrum of 4.3 in *d5*-pyridine exhibits ten resonances. Resonances assignable to the 1-adamantyl protons are observed at –5.52, -4.56, -3.62, and 3.10 ppm in a 2:1:1:1 ratio, due to the ratio of CH$_2$ to CH protons of the 1-adamantyl cage. Resonances at -50.66, -27.54, -9.34, 14.14, 32.21, and 54.69 ppm correspond to the various silylamide proton evironments.

Complex **4.3** exhibits U-$N_{Nitride}$ bonds of U1-N = 1.857(11) Å and U2-N = 2.257(11) Å with a U-N-U bond angle of 123.0(5)°. This complex is most similar to the previously reported oxy-nitrido structure, as the imido nitrogen and the O^{2-} are isolobal.[39] The isolobal nature of the imido and O^{2-} fragments would indicate that the imido should form a uranyl analogue of the N-U-N type. This is confirmed in both the U-N_{Imido} bond distance and N-U-N bond angle of 1.851(11) Å and 163.0(5)°, respectively. The shortened U-N bond distance is typical of a U-N double bond while the near linearity of the N-U-N bond angle suggests uranyl like character around this uranium center. Similarly to the oxy-nitrido, the imido-nitride can be described as a mixed valent U^{IV}/U^{VI} complex.

4.2.4 Synthesis and characterization of $U(NCPh_3)_2I_2THF_2$(4.4)

In an effort to make a uranium bis nitride complex we endeavored to utilize the reductive deprotection method utilized in the synthesis of terminal uranium oxo and sulfide complexes.[18] To explore this type of reactivity, we attempted to synthesize a uranium bis triphenylmethyl imido complex. To do this we intended to utilize a method created by the Boncella group.[22,23] To a stirring solution of UCl_4 in THF, 4 equivalents of $LiHNCPh_3$ was added (eq 4.4). After the solution stirred for approximately 6 h, one equivalent of I_2 in THF was added. The solution was stirred for 2 h and the solvent was removed in vacuo. The solid was dissolved in CH_2Cl_2 and filtered through Celite. The solution was then layered with hexanes and after 24 h at -25 °C crystals of $U(NCPh_3)I_2THF_2$ (**4.4**) precipitated from the reaction mixture in an 18 % yield.

$$UCl_4 + 4\ LiNHCPh_3 + I_2 \xrightarrow[\substack{-4\ LiCl \\ -2\ H_2NCPh_3}]{THF} U(NCPh_3)_2(THF)_2I_2 \quad (4.4)$$

Complex **4.4** crystallizes in the P21/n space group and contains two independent molecules in the unit cell. The U-N bond distances of 1.828(9) Å are typical of uranium imido bond distances.[24,40,41] The N-C bond distance of 1.53(1) Å is similar to other N-C bond distances in other imido complexes. The molecule has an octahedral geometry around the uranium center and the iodides are in the trans position in the equatorial plane.

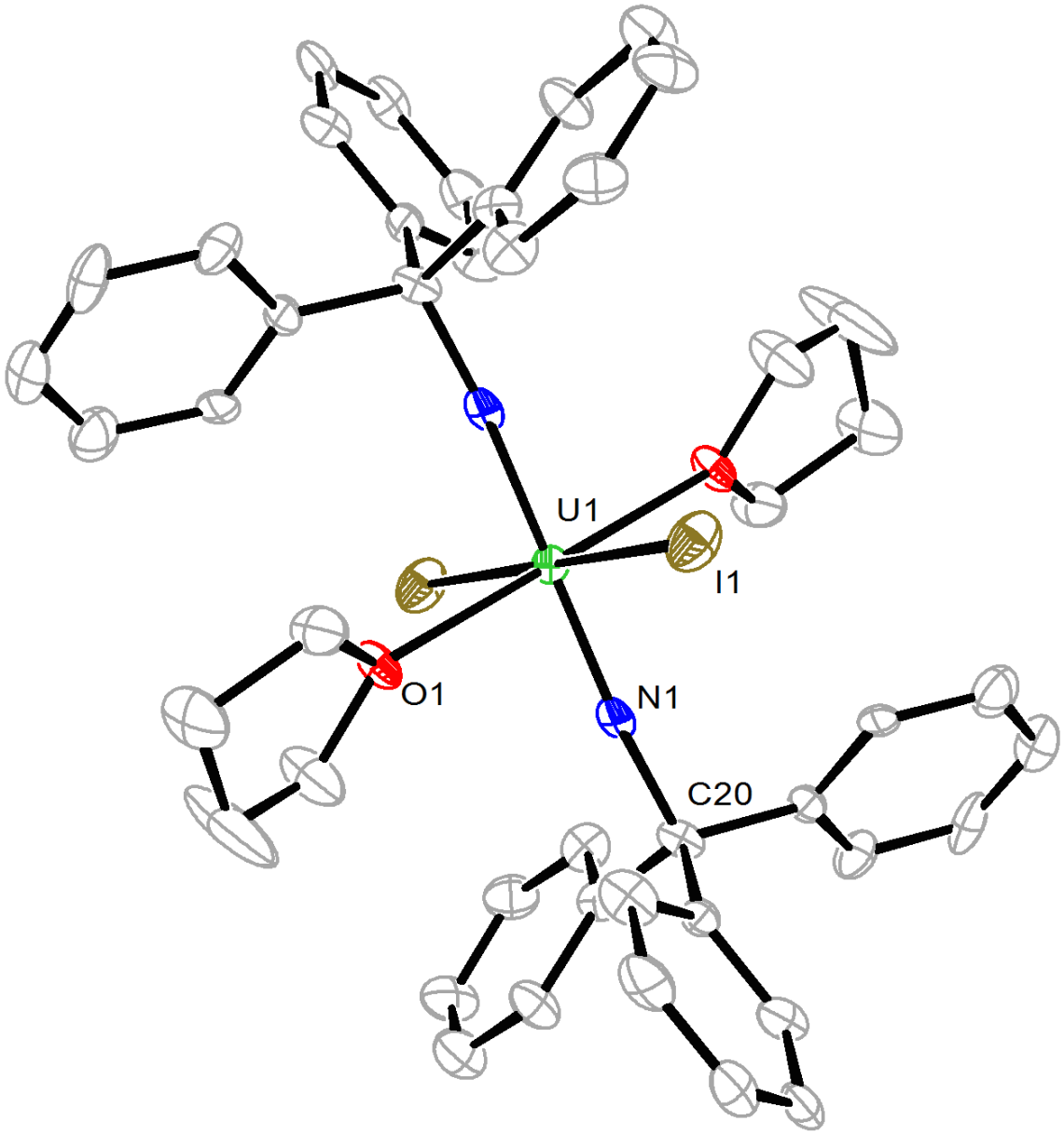

Figure 4.4 ORTEP diagram of $U(NCPh_3)_2I_2THF_2$ (**4.4**) with 20% probability ellipsoids. Selected Bond lengths (Å) and angles (°): U1-N1: 1.828(9); N1-C20: 1.526(16); U1-O1: 2.420(7); U1-I1: 3.0346(9); N1-U1-N1: 180.0; O1-U1-O1: 180.0(3); N1-U1-O1:92.4(3); I1-U1-I1: 180.0

The effort to synthesize the bis nitride complex from complex utilizing reductive deprotection did not work. Upon reacting complex **4.4** with multiple equivalents of potassium graphite no formation of the expected triphenylmethyl anion was observed. It has been suggested previously the nitrogen-carbon bond in the triphenylmethyl imido complex is too strong for reductive cleavage.[38]

4.2.5 Synthesis and characterization of $U(NCPh_3)_2(bipy)I_2$ (4.5)

Due to difficulties in the purification of complex **4.4** an attempt to make the bis trityl imido complex with an equatorial ligand was made. Similar to another bis imido synthesis made by the Boncella group, bipyridine (bipy) was utilized as a co-ligand. [42] Similar to complex **4.4,** to a stirring solution of UCl_4 in THF, one equivalent of bipy in THF was added. After stirring for 15 min, 4 equivalents of $LiHNCPh_3$ was added. After the solution stirred for approximately 6 h, 1 equiv of I_2 in THF was added (eq 4.5). The solution was stirred for 2 hours and then the solvent was removed in vacuo. The resulting solid was dissolved in CH_2Cl_2 and filtered through Celite. The solution was then layered with hexanes and after 24 hrs at -25 °C crystals of $U(NCPh_3)I_2THF_2$ (**4.5**) were isolatedin 26% yield.

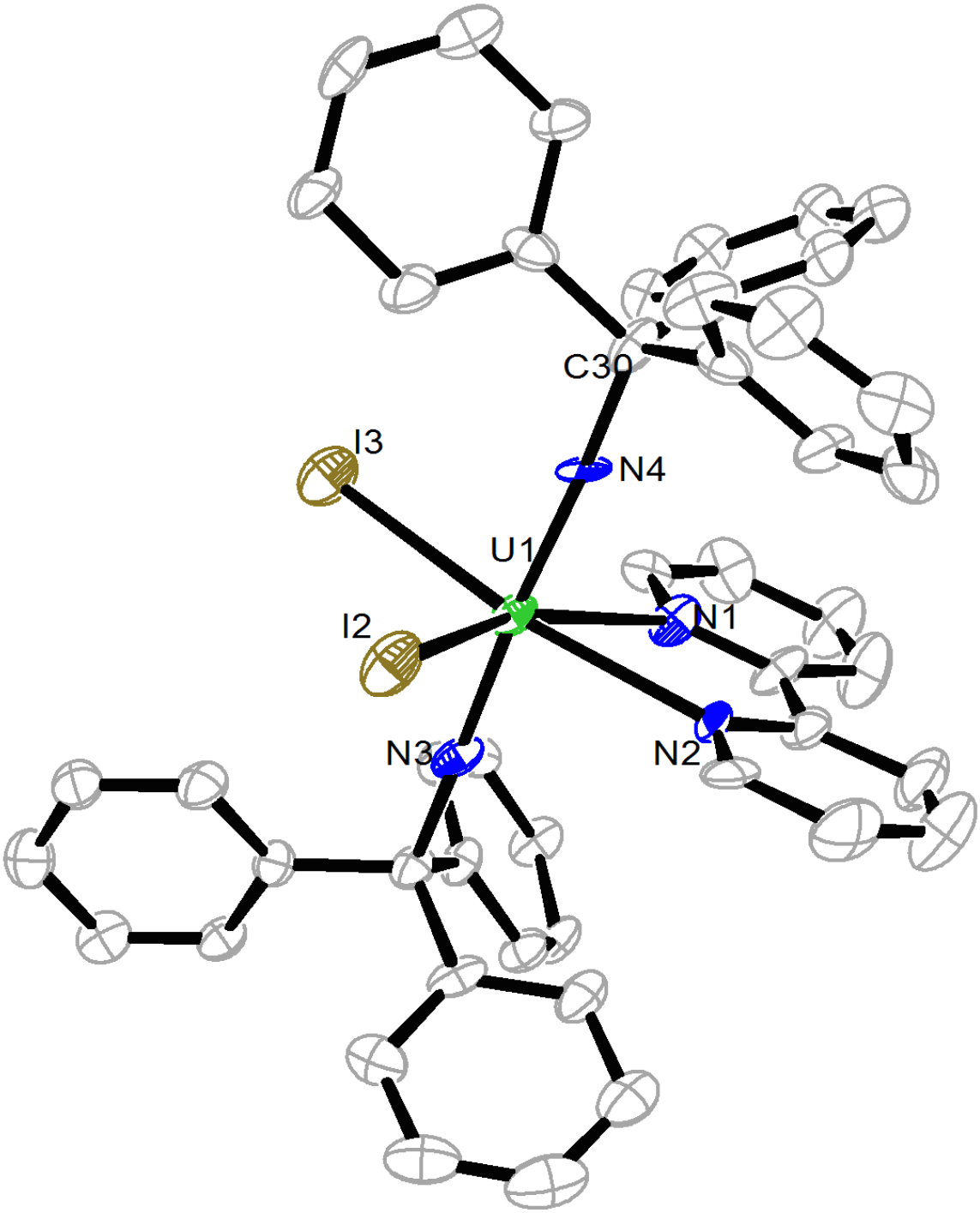

Figure 4.5 ORTEP diagram of $U(NCPh_3)_2(bipy)I_2$ (**4.5**)with 20% probability ellipsoids. Selected Bond lengths (Å) and angles (°):U1-N1:2.496(10); U1-N2: 2.535(10); U1-N3: 1.830(11); U1-N4: 1.832(10); U1-I2: 3.0252(14); U1-I3: 2.9828(15); N3-U1-N4: 174.1(4); I2-U1-I3: 103.77(5); N1-U1-N2: 63.3(3)

Complex **4.5** crystallizes in the P-1 space group and has two independent molecules in the unit cell. The U-N_{Imido} bond distances of 1.830(11) and 1.832(10) Å are typical of uranium imido complexes. The U-N_{bipy} bond distances of 2.496(10) and 2.535(10) Å are typical of coordinated neutral bipy. The iodides are in the cis position and have bond distances of 2.9828(15) and 3.0252(14) Å.

$$UCl_4 + 4\,LiNHCPh_3 + I_2 \xrightarrow[\substack{-4\,LiCl \\ -2\,H_2NCPh_3}]{\substack{THF \\ 2,2\text{- bipy}}} U(NCPh_3)_2(2,2\text{-bipy})I_2 \quad (4.5)$$

4.2.6 Synthesis and characterization of $[K(18\text{-crown-}6)]_3[P_7]$(4.6)

In an effort to synthesize new uranium phosphinidenes and phosphides we endeavored to find new phosphorus transfer reagents. Recently the Hayton group synthesized a terminal selenide and telluride utilizing polychalcogens. Using polychacogens they were able to selectively transfer selenium and tellurium.[19] In an effort to do analogous chemistry with phosphorus we endeavored to synthesize polyphosphides. Polyphosphides have been studied for several decades and were originally synthesized in the solid phase.[43-48] Recently several polyphosphides have been synthesized in a liquid ammonia synthesis.[43,49-58] There are several polyphosphides that have been confirmed including P_4^{2-}, P_7^{3-}, and P_{11}^{3-}. These complexes have not been synthesized in organic solvents, so the first step in this process is to synthesize a polyphosphide using ambient conditions.

To a stirring solution of 7 equiv of P_4 in THF, a solution containing 12 equiv of 18-crown-6 was added. After approximately 5 minutes, 12 equivalents of potassium

graphite were added to the solution. The solution turned a deep orange color with lots of solid in suspension. After approximately 4 h the solution was filtered through Celite leaving a black tacky plug. This plug was rinsed with multiple washes of pyridine and this pyridine solution was layered with diethyl ether. After 2 days at -25 °C yellow-orange hexagonal plate crystals were deposited. After analysis with X-ray crystallography the structure was determined to be $[K(18\text{-crown-}6)]_3[P_7]$ (**4.6**) (eq 4.6).

$$7P4 + 12KC8 + 12\ 18\text{-crown-}6 \xrightarrow{THF} 4\ [K(18\text{-crown-}6)]_3[P_7] \quad (4.6)$$

Complex **4.6** crystallizes in the R3 space group and contains 9 independent molecules in the unit cell. The complex contains the P_7^{3-} cluster, which has three phosphorus atoms making a triangular base, three phosphorus atoms forming a second layer and an apical phosphorus atom. The 18-crown- 6 encapsulated potassium counter ions each are coordinated to a pentagonal face of the P_7^{3-} cluster. This structure is isostructural to previously reported structures of the P_7^{3-}.[43,53,58]

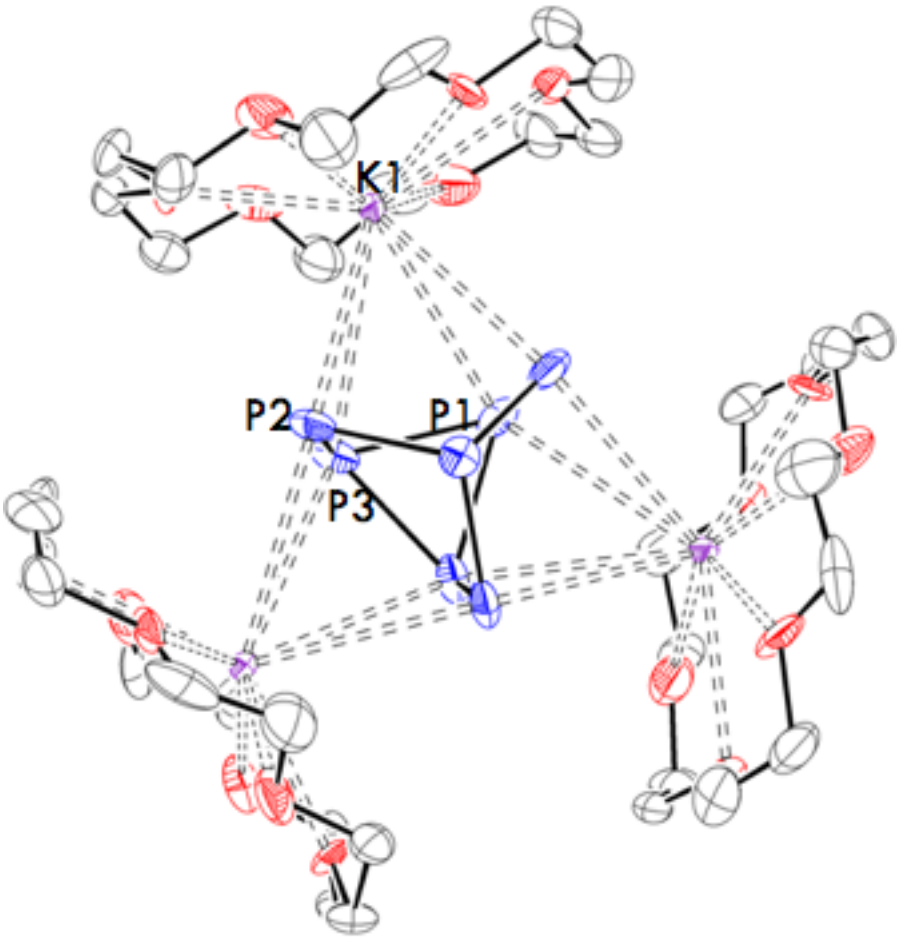

Figure 4.6 ORTEP diagram of $[K(18\text{-crown-6})]_3[P_7]$ (**4.6**)with 20% probability ellipsoids. Selected Bond lengths (Å) and angles (°): P1-P2: 2.166(6); P2-P3: 2.129(7); K1-P2: 3.337(6); K1-P3: 3.573(6)

The ^{1}H NMR spectrum of complex **4.6** exhibits a single peak at 3.46ppm corresponding to the protons on the 18-crown-6. In the phosphorus NMR there is a single peak at 218 ppm corresponding to all seven phosphorus atoms. In the solid state the phosphorus atoms are in a 3:3:1 ratio, however in the liquid state all seven atoms are equivalent and exchange with each other. This has been previously reported and demonstrated in variable temperature NMR studies of P_7^{3-}.[43]

4.2.7 Synthesis and characterization of [K(18-crown-6)][(((SiMe$_3$)$_2$N)$_3$U)$_2$(μ-η^2:η^2-P$_2$)](4.7)

To a cold solution of U[NR$_2$]$_3$ (R= SiMe$_3$) in THF, 0.33 equivalents of complex **4.6** in pyridine was added drop-wise. The solution turned a brown color and was stirred for two hours. The solvent was removed in vacuo and the solid was dissolved in Et$_2$O. The solution was layered with hexanes and after 24 hrs at -25°C small brown crystals were deposited. After analysis with X-ray crystallography the structure of [K(18-crown-6)][((R$_2$N)$_3$U)$_2$(μ-η^2:η^2-P$_2$)] (**4.7**) was obtained (Scheme 4.7).

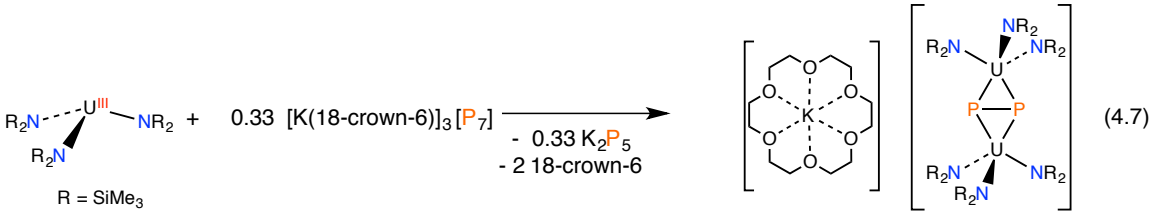

(4.7)

Complex **4.7** crystallizes in the monoclinic space group P21/c. The solid state molecular structure of complex **4.7** consists of two U[N(SiMes)]$_3$ fragments bridged by a (μ-η^2:η^2-P$_2$). The P-P bond length in **4.7** (P1-P2 = 2.184(4)) is similar to those observed in other (μ-η^2:η^2-P$_2$) complexes of the transition metals. Interestingly the U-P bonds exhibit a noticeable asymmetry. For example, the shorter bond distances are U1-P1 = 2.740(3) and U2-P1 = 2.751(3), and the longer bond distances U1-P2 = 2.876(3) and U2-P2 = 2.882(3). An anionic charge on one phosphorus and a dative bond with the other phosphorus could explain the shorter bond distances to P1.

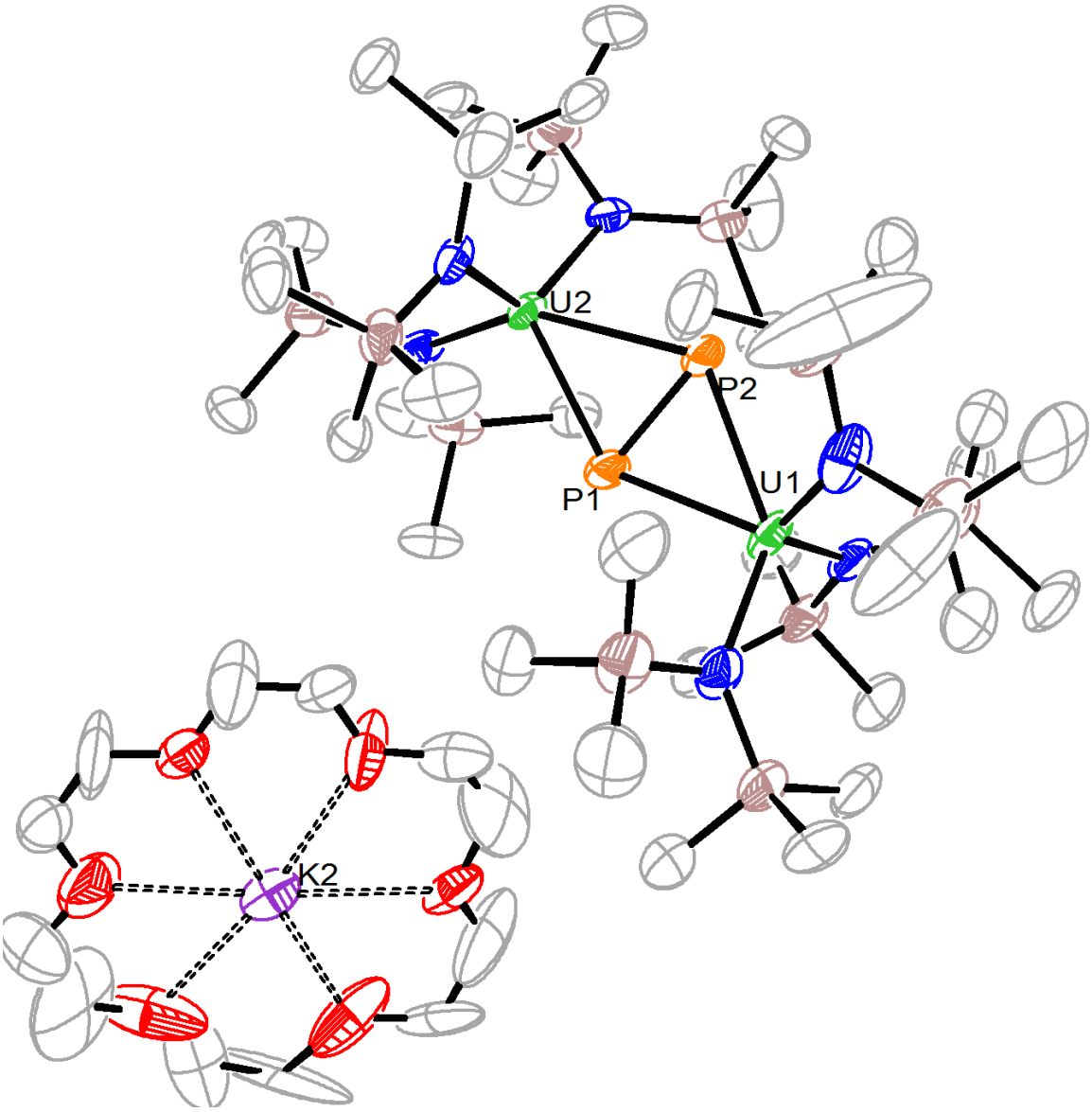

Figure 4.7 ORTEP diagram of K(18-crown-6)][$(R_2N)_3U)_2$ (μ-η^2:η^2-P_2)] (**4.7**) with 20% probability ellipsoids. Selected Bond lengths (Å) and angles (°): U1-P1: 2.740(3); U1-P2 2.876(3); U2-P1: 2.751(2); U2-P2: 2.882(3); P1-P2: 2.184(4); P1-U1-P2: 45.70(8)

4.2.8 Synthesis and characterization of [K(2,2,2-cryptand)][$((SiMe_3)_2U)_2$(μ-η^5:η^5-P_5](4.8)

To a cold solution of $U[NR_2]_3$ (R= $SiMe_3$) in Et_2O, a solid one-half equivalents of complex **4.6** was added. The solution turned a deep brown color with a brown precipitate. The solution was filtered resulting in a brown solution. A solution of 2,2,2-cryptand in Et_2O was layered on top of the brown solution and stored at 25 °C overnight. Brown crystals were deposited on the bottom of the reaction vial. The crystal was characterized with X-ray crystallography and it was found to be $[K(2,2,2\text{-cryptand})][((R_2N)_2U)_2(\mu\text{-}\eta^5\text{:}\eta^5\text{-}P_5]$ (**4.8**) (Scheme 4.8).

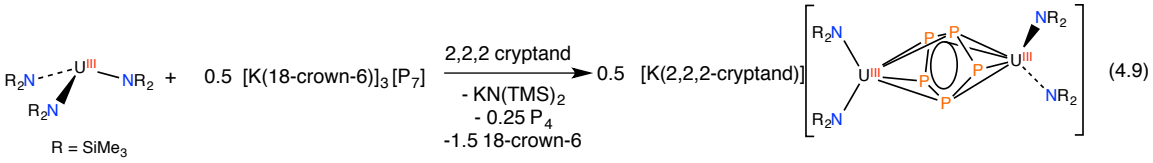

Complex **4.8** crystallize in the triclinic space group P-1. The complex has two $U[NR_2]_2$ fragments bridged by a $(\mu\text{-}\eta^5\text{:}\eta^5\text{-}P_5)$ fragment. An amide ligand from each uranium center has been release as the potassium amide salt. The P_5 fragment is not a planar cyclopentaphosphine as is expected for this ligand. The bending from the plane indicates that the ligand is no longer aromatic and more electrons have been inserted into the ring. Due to the distortion of the cyclopentaphosphine ring the U-P bond distances range from 2.374 to 3.156 Å. The P-P bond distances of 2.22 Å are elongated from the normal cyclopentaphosphine. From the bond distances and the distortion from planarity, we hypothesize the both uranium centers are U^{III} and the P_5 ligand has a charge of -3.

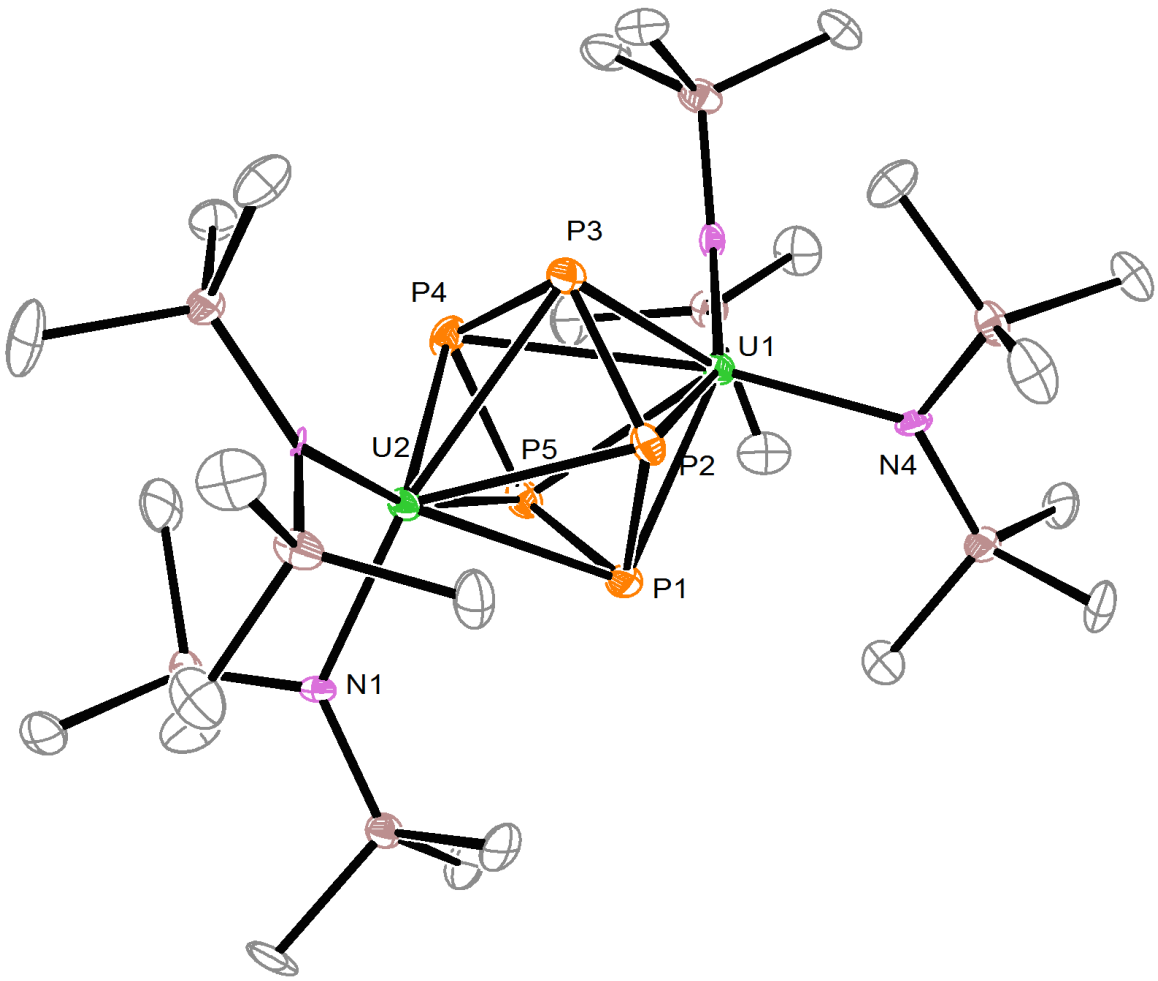

Figure 4.8 ORTEP diagram of [K(2,2,2-cryptand)][$((R_2N)_2U)_2(\mu\text{-}\eta^5\text{:}\eta^5\text{-}P_5$](**4.8**) with 20% probability ellipsoids. [K(2,2,2-cryptand)] omitted for clarity. Selected Bond lengths (Å) and angles (°): U1-P1: 2.977(4); U1-P2: 2.948(4); U2-P1: 2.811(4); U2-P2: 2.783(4); U2-P3: 3.100(4); U2-N1: 2.305(11); U1-N3: 2.298(12); P1-P2: 2.213(6); P3-P4: 2.195(6); N2-U2-N1: 100.4(4)

4.3 Summary

The reactivity of $[Na(DME)_3][(N(SiMe_3)_2)_2U(\mu\text{-}N)(CH_2SiMe_2\mathit{N}(SiMe_3))U(N(SiMe_3)_2)_2]$ with Se and Te exhibited did not form the expected analogue to the previously synthesized oxy-nitrido. The formation of the

chalcogen inserted complexes **4.1** and **4.2** were unexpected, but not unprecedented for metallacycle complexes. This simply shows that there is still a wealth of reactivity that can be explored with $[Na(DME)_3][(N(SiMe_3)_2)_2U(\mu\text{-}N)(CH_2SiMe_2\mathit{N}(SiMe_3))U(N(SiMe_3)_2)_2]$. This is evidenced by the synthesis of complex **4.3**. The exploration of uranium pnictogen was continued with the synthesis of two uranium bis imido complex **4.4** and **4.5**. These complexes were synthesized in an attempt to make a uranium bis nitride complex. Unfortunately the C-N bond could not be cleaved. To expand the chemistry of actinides and pnictogens we began to explore a new way to synthesize a uranium-phosphorus multiple bonds. Inspired by recent work with polychalcogenides, we endeavored to use polyphosphides as a phosphorus source. The first step was the room temperature synthesis of a polyphosphide, complex **4.6**, in an organic solvent. Complex **4.6** was then reacted with a uranium tris amide and produced two products, two uranium centers bridged by a P_2 fragment (**4.7**) and two uranium centers bridged by a P_5 fragment (**4.8**). While the polyphosphide **4.6** did not transfer single phosphorus atoms as intended, it has proven to be a good source of charged phosphorus.

4.4 Experimental

4.4.1 General

All reactions and subsequent manipulations were performed under anaerobic and anhydrous conditions under an atmosphere of nitrogen. Hexanes, diethyl ether (Et_2O), tetrahydrofuran (THF), and toluene were dried using a Vacuum Atmospheres DRI-SOLV Solvent Purification system and stored over 3Å sieves for 24 h prior to use. Dimethoxyethane (DME) was distilled from sodium benzophenone ketyl and stored over

3Å molecular sieves for 24 h prior to use. Pyridine, benzene-*d6*, pyridine-*d*5, and tetrahydrofuran-*d8* were dried over 3Å molecular sieves for 24 h prior to use. $UO_2Cl_2THF_2$ and $UO_2[N(SiMe_3)_2]_2THF_2$ was synthesized according to the previously reported procedures. All other reagents were purchased from commercial suppliers and used as received.

NMR spectra were recorded on a Varian UNITY INOVA 400, a Varian UNITY INOVA 500 spectrometer, or a Varian UNITY INOVA 600 MHz spectrometer. ^{1}H and $^{13}C\{^{1}H\}$ NMR spectra were referenced to external $SiMe_4$ using the residual protio solvent peaks as internal standards. IR spectra were recorded on a Nicolet 6700 FT-IR spectrometer with a NXR FT Raman Module. UV-Vis / NIR experiments were performed on a UV-3600 Shimadzu spectrophotometer. Elemental analyses were performed by the Micro-Mass Facility at the University of California, Berkeley.

4.4.2 Synthesis of [Na(18-crown-6)][$(N(SiMe_3)_2)_2U(\mu$-N)(*Se*$CH_2SiMe_2N(SiMe_3))U(N(SiMe_3)_2)_2$] (4.1)

To a brown, stirring solution of $Na(DME)_3][(N(SiMe_3)_2)_2U(\mu$-N)($CH_2SiMe_2N(SiMe_3))U(N(SiMe_3)_2)_2$] (0.1092g, 0.069mmol) in DME (4mL), was added Se powder (0.0055g, 0.069mmol). This solution was allowed to stir for 3 h, whereupon this brown solution was concentrated in vacuo to an oil. The oil was dissolved in Et_2O (3mL) and filtered through a Celite column supported on glass wool (0.5 cm × 3 cm). 18-crown-6 **(**0.018, 0.069mmol) in 3ml Et_2O was added to the solution and stirred for 3 h. The volume of the brown filtrate was reduced to (1mL) in vacuo and subsequently layered with hexanes (4mL). This solution was stored at -25 °C for 24 h,

which resulted in the deposition of dark brown rectangular crystals. (0.0460, 42% yield) **(b.)** To a brown, stirring solution of **(1)** (0.0736g, 0.046mmol) and 18-crown-6 (0.0143g, 0.054mmol) in DME (2mL), was added solution of triphenylphosphine selenide (0.0159g, 0.051mmol) dissolved in DME (1mL). This solution was allowed to stir for 3 hours, whereupon this brown solution was filtered through a Celite column supported on glass wool (0.5 cm × 3 cm). The volume of the brown filtrate was reduced to 1mL in vacuo and subsequently layered with pentane (5mL). This solution was stored at -25 °C for 24 h, which resulted in the deposition of dark brown rectangular crystals.(0.0398g, 54% yield)

4.4.3 Synthesis of [Na(18-crown-6)][$(N(SiMe_3)_2)_2U(\mu$-N)(*Te*$CH_2SiMe_2N(SiMe_3))U(N(SiMe_3)_2)_2$] (4.2)

To a brown, stirring solution of **(1)**(0.0985g, 0.062mmol) and 18-crown-6 (0.0181g, 0.068mmol) in DME (2mL), was added Te powder (0.0083g,mol) and 10µL of triethylphosphine. This solution was allowed to stir for 3 hours whereupon this brown solution was filtered through a Celite column supported on glass wool (0.5 cm × 3 cm). The volume of the brown filtrate was reduced to (1mL) in vacuo and subsequently layered with pentane (5mL). This solution was stored at -25 °C for 24 h, which resulted in the deposition of dark brown rectangular crystals. (0.0598, 59% yield)

4.4.4 Synthesis of [Na(18-crown-6)][$(N(SiMe_3)_2)_2(C_{10}H_{15}N)U(\mu$-N)($CH_2SiMe_2N(SiMe_3))U(N(SiMe_3)_2)_2$] (4.3)

To a brown, stirring solution of **(1)**(0.0753g, 0.048mmol) and 18-crown-6 (0.0156g, 0.059 mmol**)** in DME (2 mL), was added 1-azidoadamantane (0.0085g, 0.048mmol) dissolved in DME (1.5mL). This solution was allowed to stir for 3 h, whereupon this

brown solution was filtered through a Celite column supported on glass wool (0.5 cm × 3 cm). The volume of the red-green filtrate was reduced to 1mL in vacuo and subsequently layered with pentane (5mL). This solution was stored at -25 °C for 48 h, which resulted in the deposition of red-green rectangular crystals. (0.0205g, 26% yield)

4.4.5 Synthesis of $U(NCPh_3)_2I_2THF_2$(4.4)

To a stirring solution of UCl_4 (0.0951 g, 0.250 mmol) in THF (3 mL) a solution of LiNHCPh3 (0.2665 g, 1.001 mmol) in THF was added. The solution stirred for 4 hours and turned a deep brown color. After 4 hours a solution of I_2 (0.1002 g, 0.395 mmol) in THF (2 mL). The solution immediately began to gain a red tinge. After two hours of stiffing there is a brown precipitate present and a deep red brown solution. The solution was then pumped to dryness in vacuo and dissolved in 15mL of toluene. The solution was then filtered through a Celite column supported on glass wool (0.5 cm × 3 cm). The solution was then stored for 48h at -25°C which resulted in the deposition of red rectangular crystals. (0.0532g, 17.7% yield)

4.4.6 Synthesis of $U(NCPh_3)_2(bipy)I_2$ (4.5)

To a stirring solution of UCl_4 (0.0215g, 0.0566 mmol) 379.84in THF (2 mL) a solution of 2,2 bipyridine (0.0088g, 0.056 mmol) in THF (1 mL) was added. The solution stirred for 15 min and turned a pale green color. A solution of $LiNHCPh_3$ (0.0603g, 0.2265 mmol) in THF (3 mL) was added to the stirring solution. The solution stirred for 4 hrs and turned a brown color with a brown precipitate. To this solution, a solution of I_2 (0.0144g, 0.567 mmol) in THF (2 mL) was added. The solution was stirred for 2hrs and turned a deep red color with a brown precipitate. The solution was pumped to dryness in vacuo and dissolved in toluene (18 mL). The solution was filtered through a Celite

column supported on glass wool (0.5 cm × 3 cm). The solution was concentrated in vacuo to 10mL and was stored at -25°C for 48 h and red block crystals were recovered. (0.0176g, 26%yield)

4.4.7 Synthesis of $[K(18\text{-crown-6})]_3[P_7]$(4.6)

To a solid P_4 (0.1917g, 1.547 mmol) a solution of 18-crown-6 (0.8286g, 3.137 mmol) in THF (12mL) was added. This solution was stirred and solid KC_8 (0.4532g, 3.351 mmol) was added to the solution. The solution was stirred for 18hrs and the solution turned a deep orange color. The solution was filtered through Celite on a glass frit. The THF solution was discarded and 10 mL of pyridine was passed through the black plug on the filter. A deep orange solution was collected and vacuum concentrated to 8mL. This solution was layered with 10mL of diethyl ether and stored at -25°C for 72hrs. This resulted in the deposition of yellow needles and yellow hexagonal crystals. (0.4169g, 45% yield) ^{1}H NMR (400MHz, 22°C, pyridine-d_5): 3.46 (s,24H, CH_2) ^{31}P NMR (400MHz, 22°C, pyridine-d5): 218.1(s, 7P, P_7)

4.4.8 Synthesis of of $[K(18\text{-crown-6})][((SiMe_3)_3U)^2(\mu\text{-}\eta^2\text{:}\eta^2\text{-}P_2]$(4.7)

To a stirring slurry of $[K(18\text{-crown-6})]_3[P_7]$ (0.0765g, 0.068 mmol) in diethyl ether at room temperature a solution of $U[N(SiMe_3)_2]_3$ (0.1397g, 0.194 mmol) in diethyl ether was added. The solution immediately tuned a brown color and a brown precipitate formed. The olution stirred for 1hr then was filtered through a Celite column supported on glass wool (0.5 cm × 3 cm), leaving a black plug. This plug was dissolved in THF (4mL) and layered with Et_2O (3mL) and stored at -25 °C. This resulted in the deposition of brown needles (0.0162g, 9% yield).

4.4.9 Synthesis and characterization of [K(2,2,2-cryptand)][$((SiMe_3)_2U)^2(\mu\text{-}\eta^5\text{:}\eta^5\text{-}P_5$](4.8)

To a solution of $U[N(SiMe_3)_2]_3$ (0.054g, 0.075mmol) in Et_2O (4mL), solid complex 4.6 was added (0.282g, 0.025 mmol). The solution stirred for 1h turned a deep brown color and some orange-brown precipitate. The solution was filtered through a Celite column supported on glass wool (0.5 cm × 3 cm). The solution was concentrated in vacuo to 2mL. A solution of 2,2,2 cryptand (0.0094g, 0.025mmol) in Et_2O (0.5mL) was layered on top of the brown solution and stored at -25°C for 16 h. this resulted in the deposition of brown rhomboid crystals (0.0029g, 5% yield) ^{1}H NMR(400MHz, 22°C, pyridine-d5): -8.80 (s,72H, Si*Me*$_3$); 2.24 (s, 12H, C*H*$_2$); 3.30 (s, 12H, C*H*$_2$); 3.64 (s, 12H, C*H*$_2$)

4.4.10 X-Ray Crystallography

Data for complexes **4.1**, **4.2**, **4.3**, **4.4**, **4.5**, **4.6**, **4.7**, and **4.8** were collected on a Bruker KAPPA APEX II diffractometer equipped with an APEX II CCD detector using a TRIUMPH monochromator with a Mo Kα X-ray source (α = 0.71073 Å). The crystals were mounted on a cryoloop under Paratone-N oil, and all data were collected at 100(2) K using an Oxford nitrogen gas cryostream. Data were collected using ω scans with 0.5° frame widths. Frame exposure for complex **4.2** was 5s. Frame exposure for complex 4.3 was 20s. Frame exposure for complex **4.4** was 60s. Frame exposure for complex **4.5** was 5s. Frame exposure for complex **4.6** was 25s. Frame exposure for complex **4.7** was 20s. Frame exposure for complex **4.8** was 20s Data collection and cell parameter determination were conducted using the SMART program.[59] Integration of the data frames and final cell parameter refinement were performed using SAINT software.[60] Absorption correction of the data was carried out using the multi-scan method

SADABS.[61] Subsequent calculations were carried out using SHELXTL.[62] Structure determination was done using direct or Patterson methods and difference Fourier techniques. All hydrogen atom positions were idealized, and rode on the atom of attachment. Structure solution, refinement, graphics, and creation of publication materials were performed using SHELXTL.[62]

	4.1	**4.2**	**4.3**	**4.4**
empirical formula	$C_{60}H_{100}N_{10}NaO_{10}SeSi_{10}U_2$	$C_{46}H_{123}N_6NaO_8Si_{10}TeU_2$	$C_{52}H_{132}N_7NaO_6Si_{10}U_2$	$C_{46}H_{46}I_2N_2O_2U$
Crystal habit, color		block, brown	block, red-green	block, red
Crystal size (mm)		0.1 × 0.05 × 0.05	0.1 × 0.08 × 0.05	0.1 ×
Space group	P 21/n	P-1	P2(1)/c	P 21/n
volume	3866.1(16)	3899.5(7)	8479.3(10)	2560.1(14)
a (Å)	15.043(4)	15.1139(17)	11.4360(7)	14.5522(12)
b (Å)	15.290(4)	15.1224(17)	16.4482(11)	9.4115(8)
c(Å)	17.420(4)	17.6771(19)	45.235(3)	19.1734(18)
α (deg)	90.997(4)	100.696(2)	90	90
β (deg)	102.474(4)	93.099(2)	94.765(4)	102.862(7)
γ (deg)	98.330(4)	99.590(2)	90	90
Z	2	2	4	4
formula weight (g/mol)	1980.41	1796.05	1731.60	1150.71
density(calculated) (Mg/m^3)	1.701	1.530	1.356	2.112
absorption coefficient (mm^{-1})	4.873	4.716	4.002	8.767
F_{000}	1958	1784	3504	1436
total no.	32019	49805	41625	14730

reflections				
unique reflections	15362	16496	18773	5252
R_{int}		0.0559	0.1003	0.1245
final R indices [I >2σ(I)]	R1=0.1398 wR2=0.3320	R1=0.0383 wR2=0.1022	R1=0.1041 wR2=0.1648	R1= 0.0580 wR2= 0.1664
largest diff. peak and hole ($e^- A^{-3}$)	6.733 to -3.225	1.990 to -2.354	2.714 to -3.671	1.292 and -1.253
GOF	1.172	1.018	1.845	0.892

	4.5-$(CH_2Cl_2)_2$	**4.6-py**	**4.7-THF**	**4.8-2 Et_2O**
empirical formula	$C_{50}H_{42}I_2Cl_4N_4U$	$C_{60}KNOP_3$	$C_{52}H_{115}KN_6O_7P_2Si_{12}U_2$	$C_{50}H_{128}KN_6O_8P_5Si_8U_2$
Crystal habit, color	block, red	plate, yellow	needle, brown	plate,brown
Crystal size (mm)	0.2 × 0.2 × 0.05			
Space group	P-1	R 3	P 21/c	P-1
volume	2365(2)	16600.5(18)	9504(2)	3594.8(3)
a (Å)	10.353(5)	23.3217(11)	26.015(4)	14.3458(6)
b (Å)	13.075(7)	23.3217(11)	16.171(2)	15.4059(6)
c(Å)	17.778(13)	35.243(2)	22.597(3)	16.9902(7)
α (deg)	88.258(13)	90	90	97.022(2)
β (deg)	87.140(14)	90	91.233(3)	93.305(2)
γ (deg)	79.845(15)	120	90	104.387(2)
Z	2	12	4	2
formula weight (g/mol)	1332.50	882.62	1850.67	1836.29
density(calculated) (Mg/m^3)	1.871	1.059	1.293	1.459
absorption	5.002	0.218	3.670	4.711

coefficient (mm^{-1})				
F_{000}	1272	5268	3704	1468
total no. reflections	21406	32947	48093	15862
unique reflections	10384	14606	19569	11277
R_{int}	0.0728	0.0750	0.0644	0.1033
final R indices [I >2σ(I)]	R1=0.0770 wR2=0.2276	R1=0.1459 wR2=0.3818	R1= 0.1356 wR2= 0.1486	R1=0.1497 wR2=0.2218
largest diff. peak and hole ($e^{-}A^{-3}$)	3.845 and -4.815	5.197 to -1.305	2.411 to -1.784	4.415 to -3.985
GOF	1.022	1.796	1.757	2.274

4.5 References

(1) Wenzel, U.; Branquinho, C. L.; Herz, D.; Ritter, G. In *Actinide Separations*; Navratil, J. D., Schulz, W. W., Eds.; ACS: Washington D.C., 1980; Vol. 117.

(2) Musikas, C.; Le Marois, G.; Fitoussi, R.; Cuillerdier, C. *Properties and Uses of Nitrogen and Sulfur Donors Ligands in Actinide Separations*; Navratil, J. D., Schulz, W. W., Eds.; American Chemical Society: Washington D. C., 1980.

(3) Grant, G. R.; Morgan, W. W.; Mehta, K. K.; Sargent, F. P. In *Actinide Separations*; Navratil, J. D., Schulz, W. W., Eds.; ACS: Washington D.C., 1980; Vol. 117.

(4) Benedict, G. E. In *Actinide Separations*; Navratil, J. D., Schulz, W. W., Eds.; ACS: Washington D.C., 1980; Vol. 117.

(5) King, R. B. *Inorg. Chem.* **1992**, *31* (10), 1978–1980.

(6) Modolo, G.; Odoj, R. *J. Alloys Compounds* **1998**, *271–273* (0), 248–251.

(7) Ionova, G.; Ionov, S.; Rabbe, C.; Hill, C.; Madic, C.; Guillaumont, R.; Krupa, J. C. *Solv. Extr. Ion. Exch.* **2001**, *19* (3), 391–414.

(8) Shannon, R. D. *Acta Crystallogr. A* **1976**, *A32* (5), 751–767.

(9) Klaehn, J. R.; Peterman, D. R.; Harrup, M. K.; Tillotson, R. D.; Luther, T. A.; Law, J. D.; Daniels, L. M. *Inorg. Chim. Acta* **2008**, *361* (8), 2522–2532.

(10) Kozimor, S. A.; Yang, P.; Batista, E. R.; Boland, K. S.; Burns, C. J.; Clark, D. L.; Conradson, S. D.; Martin, R. L.; Wilkerson, M. P.; Wolfsberg, L. E. *J. Am. Chem. Soc.* **2009**, *131* (34), 12125–12136.

(11) Crandall, H. W. *J. Chem. Phys.* **1949**, *17*, 602–606.

(12) Bradley, D. C.; Chatterjee, A. K. *J. Inorg. Nucl. Chem.* **1959**, *12*, 71–78.

(13) McGlynn, S. P.; Smith, J. K.; Neely, W. C. *J. Chem. Phys.* **1961**, *35*, 105–116.

(14) Bombieri, G.; Croatto, U.; Forsellini, E.; Zarli, B.; Graziani, R. *J. Chem. Soc.-Dalton Trans.* **1971**, 560–564.

(15) Taylor, J. C.; Waugh, A. B. *Dalton Trans.* **1977**, No. 17, 1630–1636.

(16) Anderson, R. A. *Inorg. Chem.* **1979**, *18* (1), 209.

(17) Brown, J. L.; Fortier, S.; Wu, G.; Kaltsoyannis, N.; Hayton, T. W. *J. Am. Chem. Soc.* **2013**, *135* (14), 5352–5355.

(18) Smiles, D. E.; Wu, G.; Hayton, T. W. *J. Am. Chem. Soc.* **2014**, *136* (1), 96–99.

(19) Smiles, D. E.; Wu, G.; Hayton, T. W. *Inorg. Chem.* **2014**, *53* (19), 10240–10247.

(20) Andersen, R. A. *Inorg. Chem.* **1979**, *18* (6), 1507–1509.

(21) Cramer, R. E.; Panchanatheswaran, K.; Gilje, J. W. *J. Am. Chem. Soc.* **1984**, *106* (6), 1853–1854.

(22) Hayton, T. W.; Boncella, J. M.; Scott, B. L.; Palmer, P. D.; Batista, E. R.; Hay, P. J. *Science* **2005**, *310* (5756), 1941–1943.

(23) Hayton, T. W.; Boncella, J. M.; Scott, B. L.; Batista, E. R.; Hay, P. J. *J. Am. Chem. Soc.* **2006**, *128* (32), 10549–10559.

(24) Hayton, T. W.; Boncella, J. M.; Scott, B. L.; Batista, E. R. *J. Am. Chem. Soc.* **2006**, *128* (39), 12622–12623.

(25) Fortier, S.; Wu, G.; Hayton, T. W. *J. Am. Chem. Soc.* **2010**, *132* (20), 6888–6889.

(26) King, D. M.; Tuna, F.; McInnes, E. J. L.; McMaster, J.; Lewis, W.; Blake, A. J.; Liddle, S. T. *Nature Chem* **2013**, *5* (6), 482–488.

(27) King, D. M.; McMaster, J.; Tuna, F.; McInnes, E. J. L.; Lewis, W.; Blake, A. J.; Liddle, S. T. *J. Am. Chem. Soc.* **2014**, *136* (15), 5619–5622.

(28) Melenkivitz, R.; Mindiola, D. J.; Hillhouse, G. L. *J. Am. Chem. Soc.* **2002**, *124* (15), 3846–3847.

(29) Grundmann, A.; Sárosi, M. B.; Lönnecke, P.; Frank, R.; Hey-Hawkins, E. *Eur. J. Inorg. Chem.* **2013**, *2013* (18), 3137–3140.

(30) Duttera, M. R.; Day, V. W.; Marks, T. J. *J. Am. Chem. Soc.* **1984**, *106* (10), 2907–2912.

(31) Arney, D. S. J.; Schnabel, R. C.; Scott, B. C.; Burns, C. J. *J. Am. Chem. Soc.* **1996**, *118* (28), 6780–6781.

(32) Zanetti, N. C.; Schrock, R. R.; Davis, W. M. *Angew. Chem.-Int. Edit. Engl.* **1995**, *34* (18), 2044–2046.

(33) Fox, A. R.; Clough, C. R.; Piro, N. A.; Cummins, C. C. *Angew. Chem.-Int. Edit.* **2007**, *46* (6), 973–976.

(34) Figueroa, J. S.; Cummins, C. C. *Angew. Chem.-Int. Edit.* **2004**, *43* (8), 984–988.

(35) Stephens, F. H.; Figueroa, J. S.; Diaconescu, P. L.; Cummins, C. C. *J. Am. Chem. Soc.* **2003**, *125* (31), 9264–9265.

(36) Schnering, Von, H. G.; Hoenle, W. *Chem. Rev.* **1988**, *88* (1), 243–273.

(37) Gardner, B. M.; Balázs, G.; Scheer, M.; Tuna, F.; McInnes, E. J. L.; McMaster, J.; Lewis, W.; Blake, A. J.; Liddle, S. T. *Angew. Chem.-Int. Edit.* **2014**, n/a–n/a.

(38) Mullane, K. C.; Lewis, A. J.; Yin, H.; Carroll, P. J.; Schelter, E. J. *Inorg. Chem.* **2014**, 140811083351006.

(39) *Modern Coordination Chemistry*; Winterton, N., Leigh, G. J., Eds.; Royal Society of Chemistry: Cambridge, 2002.

(40) Spencer, L. P.; Yang, P.; Scott, B. L.; Batista, E. R.; Boncella, J. M. *C. R. Chimie* **2010**, *13* (6â€“7), 758–766.

(41) Matson, E. M.; Crestani, M. G.; Fanwick, P. E.; Bart, S. C. *Dalton Trans.* **2012**, *41* (26), 7952–7958.

(42) Jilek, R. E.; Tomson, N. C.; Shook, R. L.; Scott, B. L.; Boncella, J. M. *Inorg. Chem.* **2014**, *53* (18), 9818–9826.

(43) Turbervill, R. S. P.; Goicoechea, J. M. *Chem. Rev.* **2014**, *114* (21), 10807–10828.

(44) Dahlmann, W.; Schnering, von, H. G. *Naturwissenschaften* **1973**, *60* (9), 429–429.

(45) Dahlmann, W.; Schnering, von, H. G. *Naturwissenschaften* **1972**, *59* (9), 420–420.

(46) Schmettow, W.; Lipka, A.; Schnering, Von, H. G. *Angew. Chem.-Int. Edit. Engl.* **1974**, *13* (5), 345–345.

(47) Baudler, M.; Heum ller, R.; D ster, D.; Germeshausen, J.; Hahn, J. *Z. Anorg. Allg. Chem.* **1984**, *518* (11), 7–13.

(48) Baudler, M.; D ster, D.; Ouzounis, D. *Z. Anorg. Allg. Chem.* **1987**, *544* (1), 87–94.

(49) Korber, N.; Schnering, Von, H. G. *Chem. Ber.* **1996**, *129* (2), 155–159.

(50) Korber, N.; Daniels, J. *Z. Anorg. Allg. Chem.* **1999**, *625* (2), 189–191.

(51) Korber, N.; Daniels, J.; Schnering, Von, H. G. *Angew. Chem.-Int. Edit. Engl.* **1996**, *35* (10), 1107–1110.

(52) Korber, N.; Daniels, J. *Acta Crystallogr Sect C Cryst Struct Commun* **1996**, *52* (10), 2454–2457.

(53) Korber, N. *Phosphorus, Sulfur, and Silicon and the Related Elements* **1997**, *124* (1), 339–346.

(54) Korber, N.; Daniels, J. R. *Z. Anorg. Allg. Chem.* **1996**, *622* (11), 1833–1838.

(55) Korber, N.; Daniels, J. R. *Helv. Chim. Acta* **1996**, *79* (8), 2083–2087.

(56) Hanauer, T.; Aschenbrenner, J. C.; Korber, N. *Inorg. Chem.* **2006**, *45* (17), 6723–6727.

(57) Kraus, F.; Aschenbrenner, J. C.; Korber, N. *Angew. Chem. Int. Ed. Engl.* **2003**, *42* (34), 4030–4033.

(58) Scharfe, S.; Kraus, F.; Stegmaier, S.; Schier, A.; Fässler, T. F. *Angew. Chem.-Int. Edit.* **2011**, *50* (16), 3630–3670.

(59) 2nd ed. Bruker AXS Inc.: Madison, WI 2005.

(60) 7 ed. Bruker AXS Inc.: Madison, WI 2005.

(61) Sheldrick, G. M. University of Gottingen, Germany 2005.

(62) 6 ed. Bruker AXS Inc.: Madison, WI 2005.